Plant-induced changes mediate belowground carbon cycling in an experimentally warmed peatland

R. M. Wilson[1], C. C. Petro[2], M. M. Tfaily[3], V. G. Salmon[4], R. J. Norby[4], K. Duchesneau[2], J. Birkebak[4], K. N. Smith[1], G. Makke[3], K. E. Briley[1], S. H. Bosman[1], S. B. Hodgkins[1*], T. Song[2], N. A. Griffiths[4], S. D. Sebestyen[5], P. J. Hanson[4], C. W. Schadt[4], J. E. Kostka[2], and J. P. Chanton[1]

[1]Earth Ocean and Atmospheric Science, Florida State University, Tallahassee, FL U.S.A.

[2]School of Biology, Georgia Institute of Technology, Atlanta GA, U.S.A.

[3]Department of Environmental Science, University of Arizona, Tucson, AZ U.S.A.

[4]Environmental Sciences Division, Oak Ridge National Laboratory, Oak Ridge, TN U.S.A.

[5]Northern Research Station, U.S.D.A. Forest Service, Grand Rapids, MN U.S.A.

Corresponding author: Rachel Marie Wilson (rmwilson@fsu.edu)

*current affiliation: The Ohio State University, Columbus OH, U.S.A.

Key Points:

- Climate drivers alter plant species composition as well as the chemical composition within individual plant species
- The plant community response to climate drivers significantly changes the quantity and quality of organic matter inputs to peatlands
- These changes have consequential effects on microbially-mediated belowground greenhouse gas production

Abstract

Warming and elevated atmospheric CO_2 profoundly impact peatland ecosystems, particularly through changes in plant species composition. Plants regulate the initial input of organic compounds to peatland belowground systems, controlling the availability of electron donors and electron acceptors that fuel microbially mediated organic matter decomposition to CO_2 and CH_4. However, explicit links between porewater CO_2 and CH_4 dynamics and plant-derived chemical compounds remain relatively undefined. In a **w**hole **e**cosystem **w**arming (WEW) experiment, we investigated how warming affects plant leaf chemical composition and species assemblages, and how the alteration of leaf-derived organic compounds supplied to the subsurface impacts belowground CO_2 and CH_4 production. While earlier studies at our site found no temperature-dependent changes in CH_4 production pathways, our extended timeseries has revealed increased acetoclastic methanogenesis at higher temperatures in certain peat depths, correlated with elevated porewater phenolics. These changes appear driven by the observed increased plant productivity and altered vegetation inputs, which accelerate decomposition and fuel CH_4 production through enhanced substrate availability. We observed warming-induced changes in molecular composition both between and within plant species, suggesting that plant-mediated controls on belowground carbon processing are more complex than previously recognized.

Plain Language Summary

Climate warming and higher air carbon dioxide levels are expected to affect plant communities particularly in climate-sensitive ecosystems such as peatlands. Plants control the input of organic carbon to the belowground environment. Microbial growth in peat soils is dependent on plant-derived organic carbon inputs which result in the production of carbon dioxide and methane. In an experimentally warmed peatland ecosystem, we demonstrate the links between changing plant communities, as well as the response of individual species to warming, the belowground carbon inputs and ultimately the production of these gases. What is most interesting, is that even should the plant community remain seemingly unchanged, the chemical composition of individual plant species may be altered under warmer conditions such that greenhouse gas production is stimulated.

1 Introduction

Climate change-induced warming and elevated atmospheric carbon dioxide (CO_2) levels are expected to produce ecosystem-level effects including alteration of overall plant species composition and primary productivity of plant functional types (PFTs) as well as shifting microbial community responses that culminate in changing greenhouse gas production from vulnerable ecosystem (Wardle and Smith, 2004). Peatlands are climate-vulnerable ecosystems that contain an estimated 530-1055 Pg of organic carbon (Nichols and Peteet 2019; Hugelius et al., 2020). The majority of peatlands are located at high latitudes and are warming two to three times faster than the global average (Rintoul et al., 2018), making peatlands particularly vulnerable to climate change. As peatlands warm, their vast reservoirs of organic carbon are

likely to become increasingly susceptible to microbial decomposition converting previously stored carbon into greenhouse gases (i.e., CO_2 and CH_4; Hanson et al., 2020). CH_4 emissions from some peatlands are increasing exponentially with temperature at a faster rate than CO_2 production (Hopple et al., 2020), although stimulation of CH_4 production may be offset by warming-associated drying (Huang et al., 2021).

Currently many peatlands are active C sinks (Turetsky et al., 2007; Jones et al., 2013) because net C uptake by primary productivity exceeds C loss via heterotrophic respiration. However, climate forcings such as warming and elevated atmospheric CO_2 levels are expected to have a profound effect on the peatland C cycle, threatening their critical role as a global C sink. Primary productivity and the associated net C uptake by vegetation are stimulated by warming (Malhotra et al., 2020), a longer growing season (Natali et al., 2012) and the direct effects of elevated CO_2 on photosynthesis (Ellsworth et al., 2012). Carbon loss via heterotrophic respiration (Hicks-Pries et al., 2013) and changes in the quantity and quality of organic matter inputs (Treat et al., 2014) can be altered by temperature, which, in turn, are ultimately controlled by the chemical composition of the dominant plant species (Sutton-Grier and Megonigal 2011). Microbial decomposition and resulting greenhouse gas production is thought to be suppressed in *Sphagnum*-dominated peatlands, in part, due to the poor-quality *Sphagnum*-derived organic matter (van Breeman 1995; Turetsky 2003; Hough et al., 2021; Wilson et al., 2022; Cory et al., 2025). In addition, evidence from whole ecosystem warming (WEW) experiments suggests that whole ecosystem warming inhibits peat mosses (*Sphagnum* spp.) and stimulates the growth of shrubs (Norby et al., 2019; McPartland et al., 2020) resulting in the so-called shrubification of peatlands, which is likely to result in the input of more reactive and bioavailable soil organic matter belowground (Chanton et al., 2008; Ofiti et al., 2023; Tfaily et al., 2013; Wilson et al., 2021a, 2022). However, the impacts of climate drivers (warming and air CO_2) on plant-microbe interactions are complex and remain understudied. Although *Sphagnum* is generally thought to inhibit peat decomposition in part due to its phenolic content (Verhoeven and Liefveld 1997), other researchers have suggested that relative to *Sphagnum*, shrubs may contain higher concentrations of phenolic compounds which could suppress decomposition as *Sphagnum* cover declines (Wang et al., 2021). Lower carbon oxidation state (NOSC = nominal oxidation state of carbon) organic matter (low quality organic matter) has been correlated with increasingly methanogenic conditions (e.g., Wilson et al., 2021a), thus higher availability of organic oxygen-

rich compounds (i.e., with greater NOSC) will likely stimulate CO_2 over CH_4 production resulting in increasing CO_2:CH_4 ratios. Additionally, enhanced availability of labile organic matter is thought to favor methane production via the acetoclastic pathway over the hydrogenotrophic pathway (Chanton et al., 2008; D'Andrilli et al., 2010; Tfaily et al., 2014) suggesting a mechanism for changes in methane production pathways.

We hypothesized that: 1) both plant species composition and the chemical content of plants themselves will respond to warming, thereby increasing belowground organic matter lability (quality) and stimulating organic matter decomposition as reflected by increasing greenhouse gas production and 2) changes in soil organic matter compounds, both dissolved and derived from plant litter, could be leveraged to predict CO_2 and CH_4 production dynamics at the Spruce and Peatland Responses Under Changing Environments (SPRUCE) experimental peatland in northern Minnesota (USA; https://mnspruce.ornl.gov/; Hanson et al., 2017). The SPRUCE study provides warming and elevated CO_2 manipulated conditions to test our hypotheses. We measured changes in porewater dissolved organic matter (DOM) molecular composition and CO_2 and CH_4 production over a six-year period (2015 through 2022). Additionally, we characterized bulk chemical composition of major plant functional types to assess how plant community dynamics influence the dissolved organic matter quality and then used regression analyses to quantify the effects on CO_2 and CH_4 production as well as methanogenic pathways. Finally, we employed an amplicon sequencing approach to investigate the linkages between microbial community dynamics, plant organic matter inputs, and greenhouse gas production with warming.

2 Materials and Methods

2.1 *Site Description*

The SPRUCE experiment is located within the S1 bog of the USDA Forest Service Marcell Experimental Forest in northern MN, USA (N47°30.476'; W93°27.162'). S1 is a perched, ombrotrophic bog with an annual precipitation of 787 ± 104 mm per year and no input from the surrounding groundwater aquifer (Sebestyen et al., 2021). SPRUCE is a whole-ecosystem warming experiment combined with elevated air partial pressure of CO_2 (eCO_2) applied in a regression design—with temperature as the predictor— to test the ecosystem response to climate drivers in a non-permafrost, undrained peatland. In contrast to an ANOVA design, the regression experimental design across a broad range of temperature treatments allows the quantification of temperature response curves useful in

ecological studies (Hanson et al., 2017). Eight randomly selected enclosures across the bog are warmed up to +9°C relative to the control enclosure (+2.25, +4.5, +6.75, +9°C and the +0°C control). Warming includes both deep peat heating (initiated in June of 2014 Hanson et al., 2011; Wilson et al., 2016) and heating of the overlying air (initiated in August 2015; Hanson et al., 2017). In five of the 10 enclosures (including one control and one of each warming level), elevated air CO_2 of approximately 871-971 p.p.m.v. is also applied during the growing season beginning in June 2016. The source of the CO_2 for the eCO_2 treatment is pure CO_2 from a commercial facility with a radiocarbon-dead (-999‰) $^{14}CO_2$ and a depleted $^{13}CO_2$ (-40‰) signature. When mixed with ambient air to achieve about 900 p.p.m.v. during the growing season, the resulting mean measured isotopic values of the air in the plots were ^{14}C = -523‰ ± 32 (s.d.) and $\delta^{13}C$ = -25.7‰ ± 1.0‰ (s.d.). In the ambient CO_2 plots, ^{14}C = -33.2 ± 26.3‰ and $\delta^{13}CO_2$ = -8.3‰ ± 0.9‰ (s.d.). The enclosures are 12.8 m in diameter and surrounded by 7 m tall open-topped walls that allow for precipitation and atmospheric deposition, as well as peatland-atmosphere energy and vapor exchange (Hanson et al., 2017). The subsurface peat hydrology for each enclosure is isolated from the rest of the S1 bog by corrals that extend 3-4 m deep into the underlying lake sediment (Sebestyen and Griffiths 2016).

2.2 *Plants*

The bog where SPRUCE is located initially had an understory dominated by *Sphagnum* mosses, underlying ericaceous shrubs, graminoids and forbs (*Maianthemum trifolium*; McPartland et al., 2020; Norby et al., 2019) and two dominant tree species (*Picea mariana, Larix laricina*). Over time the exact relative compositions have been found to shift in the heated plots due to warming-induced processes (McPartland et al., 2020; Norby et al., 2019). Common species of ericaceous shrubs include *Rhododendron groenlandicum, Chamaedaphne calyculata,* and *Vaccinium angustifolium* (McPartland et al., 2020).

Aboveground plant tissue (consisting of *P. mariana, M. trifolium, R. groenlandicum, C. calyculata,* and *V. angustifolium*) and *Sphagnum* (including *S. divinum, S. angustifolium,* and *S. fallax*) were collected from each of the warming treatment enclosures during the peak growing season in years 2016, 2017, 2021, and 2022 (see Phillips et al., 2021 for details on plant collection). At the time we did not differentiate between the different species of *Sphagnum* for measurement purposes. When possible, without disturbing other experiments, replicate plant samples were collected from treatment enclosures. Aboveground biomass of tree species (*P. mariana* and *L. laricina*) was calculated based on species and site-specific allometries relating tree height and diameter at breast height to aboveground dry mass (Griffiths et al 2017; Hanson et al 2020). Aboveground biomass of understory vascular plants was measured in clip plots (up to 4 per plot, ranging from 0.25-1.15 m^2 depending on year of sampling) where

aboveground tissues were sorted by species, dried, and weighed. Please see Hanson et al., (2025) for additional details and discussion of the plant measurements (data available: Iversen et al., 2017; Hanson et al., 2018; and Norby et al., 2018). *Sphagnum* biomass was determined based on percent cover surveys (as in Salmon et al., 2021) and an assumed, arbitrary 10 cm depth of live *Sphagnum* biomass.

2.3 *Fourier Transform Infrared (FT-IR) spectroscopy*

Fourier Transform Infrared (FT-IR) spectroscopy was used to measure the chemical composition of plant species within each plot. For understory biomass clip-plot samples, all above ground plant material was removed, placed in bags, and frozen. Samples were then individually thawed and sorted by species and the leaf material was separated from other tissues. Leaf material was dried at 60–70 °C and ground to a homogenous powder. Only current growth year material was analyzed. For *Sphagnum* the aboveground visibly green (apparently alive) portions of the mosses were used, typically the top 3cm. FT-IR spectra were collected using a PerkinElmer Spectrum 100 FTIR spectrometer fitted with a CsI beam splitter and a deuterated triglycine sulfate detector. Transmission-like spectra were obtained using a Universal ATR accessory with a zinc selenide/diamond composite single-reflectance system. Each sample was placed directly on the ATR crystal, and force was applied so that the sample came into good contact with the crystal. Spectra were acquired in % transmittance mode between 4000 and 650 cm^{-1} (wavenumber) at a resolution of 4 cm^{-1}, and ten scans were averaged for each spectrum. Spectra were ATR-corrected, baseline-corrected, and then converted to absorbance mode using the instrument software. Area-normalized and baseline-corrected peak heights for common classes of compounds observed in soil organic matter were calculated using the methods and script described by Hodgkins et al., (2018). Peak assignments were derived from the literature as described in Supplemental Figure S2 and heights were calculated and baseline and area corrected using R (R Core Team 2021) as described by Hodgkins et al., (2018). Polysaccharide-like structures were identified by o-alkyl stretching at 1030 cm^{-1}. Lignin, phenolic lignin-like structures and aromatics were identified by peaks at 1265, 1515, and 1650 cm^{-1}, respectively. Waxy, aliphatic fats were identified from the region 2850 to 2920 cm^{-1}.

2.4 *Porewater Sample Collection*

Six to 12 piezometers are installed within each of the enclosures that allow porewater to be collected at depths of 25, 50, 75, 100, 150 and 200 cm with some replication. Each piezometer consists of a 2.5 cm diameter PVC (poly vinyl chloride) pipe with a screen mesh bottom installed to the previously specified depths below the peat hollow surface. Piezometers were covered, but not sealed, when not being actively sampled. Twelve hours prior to porewater sampling the piezometers were pumped until no water

flowed and then allowed to recharge. Given the small surface area of the pipes, diffusion of gases into and out of the porewater is negligible over the 12-hour recharge period as supported by finding near or slightly above saturation concentrations of gases in the deep porewater. Perforated stainless steel tubes were used to collect porewater from 10 cm when the depth of the water table allowed. Porewater samples were collected in August 2015, July 2016, and August 2017 and measured for total organic carbon (TOC), total dissolved CO_2, and CH_4 concentrations and stable isotopes ($\delta^{13}C$) as well as detailed molecular composition by Fourier transform ion cyclotron resonance mass spectrometry (FTICR-MS) in select samples. Additional porewater samples collected throughout March-December of 2018-2022 were analyzed for CO_2 and CH_4 concentrations and stable isotopes ($\delta^{13}C$) and a select number by FTICR-MS. Samples for amplicon sequencing were collected in June 2016 and August 2017.

2.5 *Organic matter quality by Fourier transform ion cyclotron resonance mass spectrometry (FTICR-MS)*

Porewater samples for FTICR-MS were immediately filtered to 0.7 μm in the field into polycarbonate sample containers and then frozen at -20°C. At the lab, samples were thawed and then diluted 2:1 with HPLC grade methanol for direct injection using a 12 T FTICR-MS (at EMSL, a DOE-BER national user facility located in Richland, WA) coupled with electrospray ionization in negative ion mode. Ion accumulation times were adjusted between 0.1 to 0.3 s to account for variation in C concentration. For each sample, 144 scans were collected, averaged, and then internally calibrated using homologous CH_2 (i.e., 14 Da separation) series. Molecular formulae were identified using Formularity software (Tólic et al., 2017) according to the Compound Identification Algorithm of Kujawinski and Behn 2006 as modified by Minor et al., 2012 using a signal:noise ratio greater than 7 and mass measurement error <1 parts per million (ppm). From the resulting FTICR-MS, we calculated biochemical compound classes based on the relative abundance of C, H, and O in each compound identified as described in Bailey et al., (2017). We divided the signal intensity for each individual compound by the sum of signal intensities for all compounds in each sample to create a normalized signal intensity for each compound. These values were summed for the major compound classes (sugars, lipids, and tannins/lignins/condensed hydrocarbons) to determine the percent each class contributed to the total sample. We also calculated the nominal oxidation state for C (i.e. NOSC; LaRowe and van Cappellen 2011; Keiluweit et al., 2016) for each of the identified compounds in each sample. NOSC provides a thermodynamically determined metric of the quality of organic matter available for decomposition (Keiluweit et al., 2016; Wilson and Tfaily 2018) under anoxic conditions. However, some high NOSC compounds may nevertheless be less bioavailable due to other limitations, such as high physical complexity of molecular structure that would tent to slow or inhibit decomposition. We observed a strong

correlation between NOSC and compounds typically considered to be less bioavailable, likely due to such physical constraints (e.g., tannins, lignins, and condensed hydrocarbons; Supplemental Figure 1). Thus, we calculated $NOSC_{np}$ for each sample as the sum of NOSC for compounds that were not phenolic (np) or condensed compounds by subtracting out the NOSC of compounds identified as tannin-like lignin-like or condensed hydrocarbons. $NOSC_{np}$ is used in correlations and figures throughout the main text.

2.6 *Phenolics*

We used the Folin-Ciolcateu (FC) method to quantify total soluble phenolic abundance, as described by Bancuta et al., (2016). Briefly, we added 0.1 mL of porewater to 0.5 mL of 0.27M FC reagent (diluted from starting concentration of 2M, obtained from VWR International, cat# IC19518690). We mixed this solution and allowed it to sit for 5 minutes before adding 0.5 mL of 93.6 g/L Na_2CO_3 solution (VWR, cat# 97061-296). The samples were once again mixed and allowed to sit for 2-3 hours. Their absorbance was then measured at 765 nm using an ultraviolet-visible (UV/Vis) absorption spectrophotometer (BioTek Synergy HTX Multi-Mode Reader). We used a standard calibration curve of gallic acid using seven concentrations ranging from 0.27 to 6.6 g/mL. Absorbance values were all blank-corrected and concentrations were adjusted based on the dilution imposed by reagent addition. The detection limit for this methodology was 2.5 µmol L^{-1}.

2.7 *CO_2 and CH_4 analyses*

Porewater samples for CO_2 and CH_4 analyses were injected into pre-evacuated serum-sealed glass vials. Phosphoric acid (1 mL, 10%) was added to each vial to preserve the samples and ensure that all DIC was in the form of dissolved CO_2. Porewater CO_2 and CH_4 concentrations and isotopes were analyzed simultaneously via headspace analysis using a Finnigan Mat Delta V Isotope Ratio Mass Spectrometer coupled to a gas chromatograph (Merritt et al., 1995). The analytical uncertainty based on repeated measurements of a standard was <0.15‰ for $\delta^{13}CO_2$ and $\delta^{13}CH_4$ and <5% for CO_2 and CH_4 concentrations. Alpha is a measure of the isotopic separation between the CO_2 and the CH_4 which can indicate the relative pathway of methane production (Whiticar 1999) and was calculated as $[(\delta^{13}CO_2 + 1000)/ (\delta^{13}CH_4 + 1000)]$. Higher values of alpha indicate methane produced by the hydrogenotrophic pathway and lower values of alpha indicate methane produced via the acetoclastic pathway (Chanton et al., 2005; Whiticar 1999). Porewater CO_2:CH_4 ratios were corrected for the differential solubility of CO_2 vs. CH_4 in water using the isotope correction method of Corbett et al., (2012) to correct for the higher diffusive loss of CH_4 relative to CO_2 in an open system.

2.8 *Microbial community composition*

Porewater samples for amplicon sequencing of the 16S rRNA gene were collected in June 2016 and August 2017. Individual samples consisted of 50-200 mL of porewater, with higher volumes collected for deeper samples due to lower microbial biomass at depth. Porewater was filtered through 0.2 µm polycarbonate filters (47 mm diameter, Whatman Nucleopore) on a Nalgene filtering apparatus immediately after sampling. The filters were stored in microcentrifuge tubes on dry ice and shipped to Georgia Institute of Technology, where they were stored at −80 °C until further processing. DNA was extracted from whole filters using the DNeasy PowerSoil Extraction Kit (QIAGEN). Amplification and sequencing of the 16S rRNA gene were performed using the universal primer pair CS1_515F (5'-ACACTGACGACATGGTTCTACA_GTGCCAGCMGCCGCGGTAA) and CS2_806R (5'-TACGGTAGCAGAGACTTGGTCT_GGACTACHVGGGTWTCTAAT) (Caporaso et al., 2011) as described in Wilson et al. (2016). For each sample, the generated amplicons were barcoded with unique 10-base barcodes (Fluidigm Corporation) and sequenced on an Illumina MiSeq2000 platform. The raw 16S rRNA gene sequences have been deposited in the National Center for Biotechnology Information (NCBI) Short Read Archive (SRA) under BioProject PRJNA640652. Sequence processing and analysis was performed using the DADA2 workflow (v.1.24; Callahan et al., 2016) in R v.4.2.0. Taxonomy was assigned to the resulting amplicon sequence variants (ASVs) using the SILVA SSU rRNA reference database (Release 138; Quast et al., 2013).

Differential abundance analysis was performed using DESeq2 (Love et al., 2014) to identify microbial groups that differed significantly between warming treatments. For this analysis, ASVs were grouped at the genus level and samples were separated according to their depth of origin. DESeq2 was run using the experimental temperature treatment as a factor, identifying microbial genera whose relative abundances were significantly higher in the +9ºC enclosures relative to the +0ºC enclosures ($p < 0.05$).

2.9 *Statistical analyses*

FT-IR peak heights were identified, calculated, and normalized using R (R Core Team 2021) as described by Hodgkins et al., (2018). To test the hypothesis that the temperature effects on plant chemical concentrations vary across plant species and chemical classes we used linear mixed-effects modeling ('fitlme' in MATLAB R2022b, MathWorks, Natick, MA, USA). Both linear and non-linear temperature responses were modeled, with the quadratic term (T^2) included as a fixed effect and its interactions with species and chemical class. Random effects of Species × Chemical × Plot × Year were included to account for repeated measures within plots across several years.

To test the hypothesis that plant chemical inputs influence porewater chemical composition, which in turn affects C gas production dynamics (CO_2, CH_4 concentration and stable isotope values), we used linear mixed-effects models within a causal chain framework. The conceptual framework (illustrated in

294 Figure 1) parallels structural equation modeling (SEM), but in a simplified sequential form to reduce
295 overfitting given our data limitations.
296

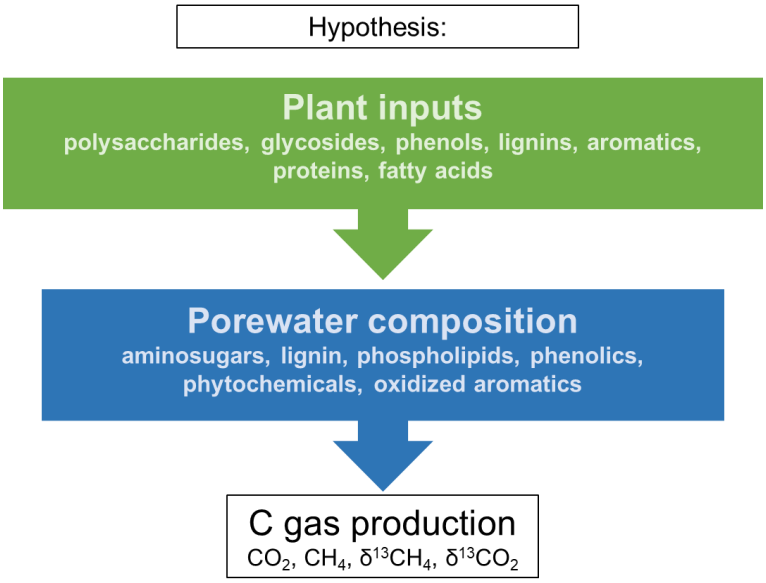

297
298 Figure 1: Schematic diagram of hypotheses tested.
299
300 The first step tested whether plant inputs predict porewater chemical abundances by modeling each
301 porewater chemical (phenolics, aminosugars, lignin, phospholipids, oxidized aromatics, and
302 phytochemicals) (at 50 cm) as a response and biomass-weighted plant inputs as the predictors. This
303 approach allowed us to account for both changes in plant chemical composition (e.g. with temperature)
304 and changes in the plant community species composition. Plot and year were treated as random effects to
305 account for repeated sampling as before. We focused on the porewater composition at 50 cm because it
306 was the most consistently sampled depth throughout the study and allowed for the most data to be
307 included. The second step modeled C gas dynamics (CO_2 concentration, CH_4 concentration, $\delta^{13}CO_2$ or
308 $\delta^{13}CH_4$) as responses, with porewater chemical composition as predictors. Fixed effects included
309 temperature, eCO_2 treatment, and depth, including all two- and three-way interactions among them.
310 Again, plot and sampling date were included as random effects to account for repeated measures and all
311 modeling was done in MATLAB using fitlme. When combined, this two-stage modeling framework
312 allowed us to evaluate indirect pathways from plant chemistry to carbon gas dynamics via porewater
313 chemistry. For all models, data was z-score standardized to accommodate unit differences. Generative
314 artificial intelligence (AI) (OpenAI, 2023) was used to assist with coding syntax in a completely
315 supervised approach where each line of code was verified and edited as needed (by RMW) for accuracy.
316 To illustrate significant interactions between plant composition, porewater and C gas dynamics we built a

network with chemicals as nodes and significant interactions as edges in Cytoscape 3.10.1 (Shannon et al., 2003; Breitling et al., 2006).

To estimate the plant inputs to the subsurface DOM pool, we multiplied the individual compound classes for each species/plot/date combination by the measured biomass. In cases where biomass estimates were missing, we used the mean value of the nearest dates for that species/plot combination. The resulting biomass-weighted inputs for each compound were then summed for all plant species per plot/date combination to get the biomass-weighted standing stocks. Since we measured the chemical compound composition of the leaves, we assumed these standing stocks were directly proportional to the chemical inputs at each plot with a lag of 1 year. Such that the standing stock biomass in 2016, for example was correlated with the porewater chemical composition measured in 2017. Although other plant tissues (e.g. roots) also contribute to the belowground chemical inputs and evergreen plants (e.g. Picea) might have longer lag periods, this approach provides a first approximation of how variation in plant chemical composition is related to belowground biogeochemical cycling. We modeled the resulting compounds values with a 3-way interaction of temperature × eCO2 treatment × chemical compound classes with plot as a random effect (using fitlme).

3 Results

3.1 Plants and FT-IR Results of Plant Chemical Composition

Tree species of the genus *Picea* comprised the largest amount of overall aboveground vascular plant biomass, followed by the shrubs *Rhododendron* and *Chamaedaphne* (Figure 2a). Significant temperature-driven trends in aboveground biomass were observed for several plant species (Figure 2). In particular, shrubs *Rhododendron* and *Vaccinium* showed a positive increase in biomass with temperature. *Maianthemum*, *Picea*, and *Sphagnum* biomass all declined with temperature.

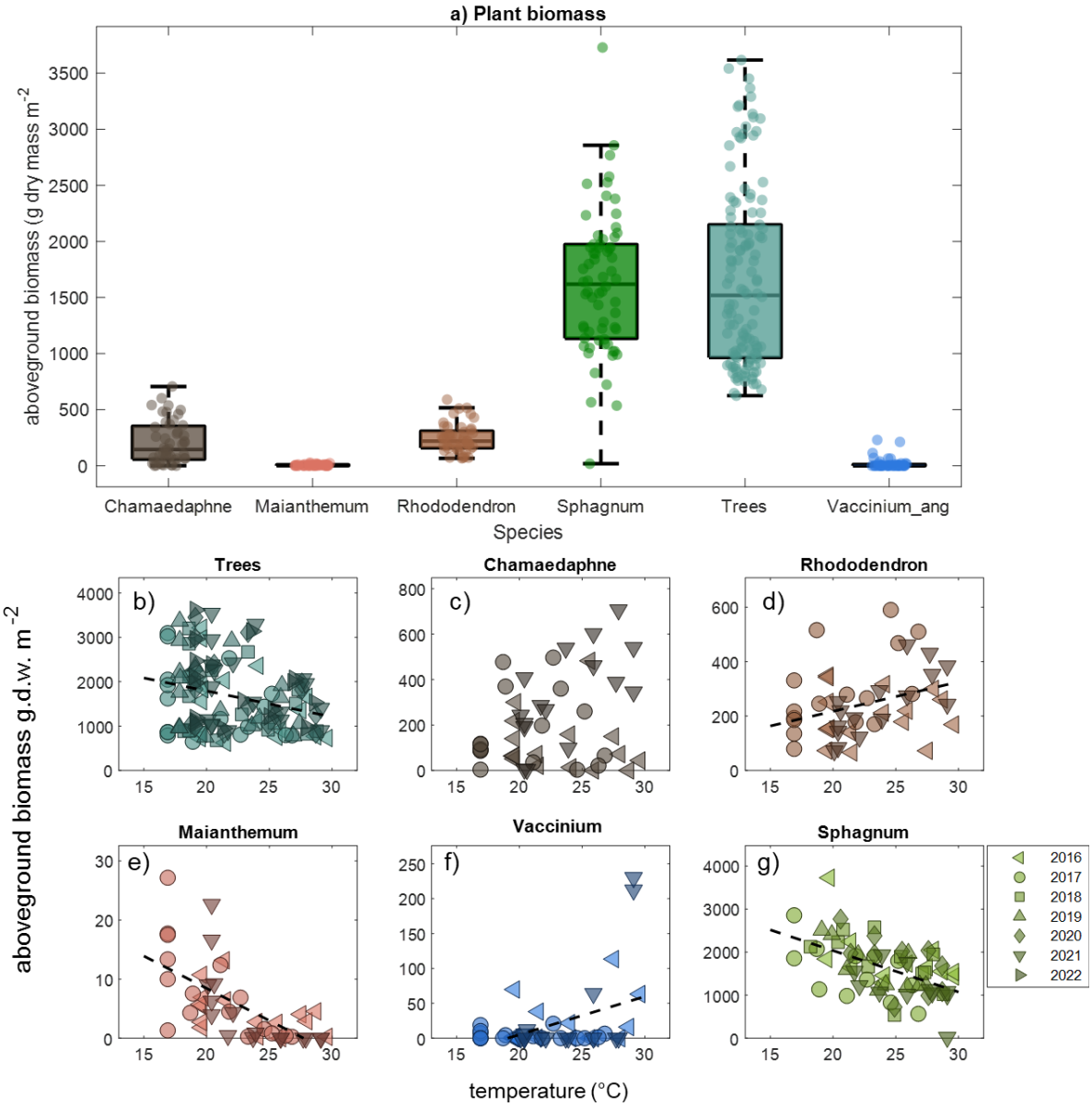

Figure 2: Panel (a) contribution of each plant species to the overall aboveground biomass (one point per chamber per year). Panels (b-g) show how major plant species change in aboveground biomass with increasing air temperature in both the ambient and elevated CO_2 treatments. Full statistical results are provided in the supplement table S1 and S2. Regression lines for aboveground biomass versus air temperature are fit across data from all years and both ambient and eCO_2. All panels with regression lines showed significant trends ($p < 0.05$).

Significant differences were observed in whole-leaf, bulk chemical composition between different plant species (Figure 3). *Sphagnum* and graminoids have relatively low aromatic content while the trees (*Picea*) and shrubs (e.g. *Vaccinium*, *Chamadaphne* and *Rhododendron*) had relatively high aromatic content (Figure 3b). In contrast, polysaccharide content was higher in *Sphagnum* and graminoids but lower in the trees and shrubs (Figure 3d). There were significant difference in phenolic

content (Figure 3c), glycosides (Figure 3e), lignin-like compounds (Figure 3f) and fatty acid (Figure 3g) content among the plant species.

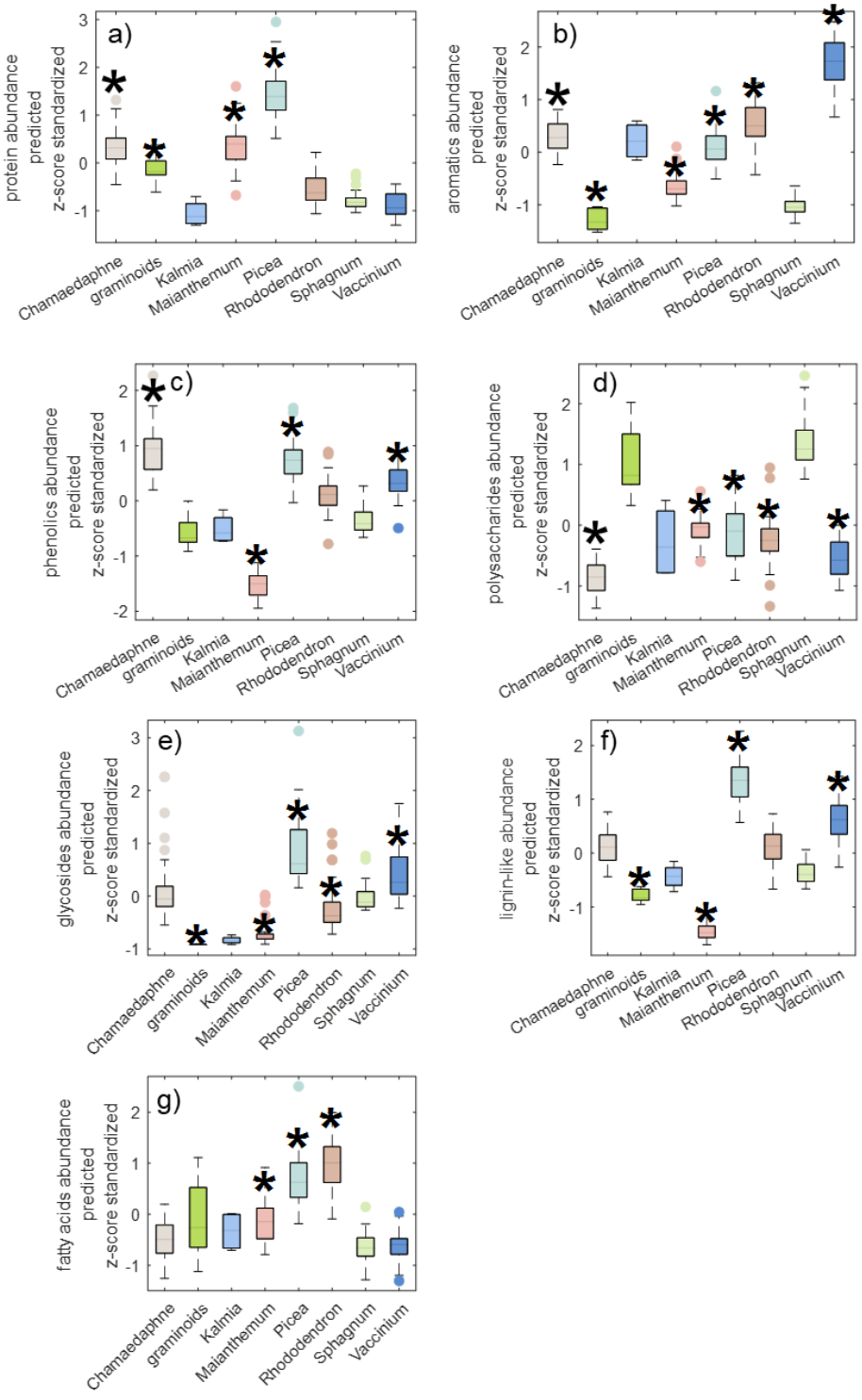

Figure 3: FT-IR based bulk compound classes in plant leaves. Results are shown as the mean ± interquartile range of FT-IR peak heights normalized to the spectral area with dots indicating outliers. Representative spectra indicating the wavenumber used for each compound class is given in the Supplement Figure 2. Significant differences from *Sphagnum* values for each compound ($p < 0.05$ as determined in the fitlme modeling) are indicated by asterisks.

We observed significant linear and non-linear temperature responses in the chemical content within plant species across the study (Figure 4). *Maianthemum* exhibited non-linear temperature declines in fatty acids (Figure 4a) and phenolics (Figure 4h) and linear declines with temperature in polysaccharide (Figure 4i) and proteins (Figure 4e). Aromatic content in *Maianthemum* increased linearly with temperature (Figure 4k). *Picea* showed linear declines with temperature in fatty acids (Figure 4b) and linear increases in polysaccharides (Figure 4j) and proteins (Figure 4f). There was a non-linear temperature response of aromatic content in *Picea* (Figure 4l). *Rhododendron* exhibited linear declines in fatty acids (Figure 4c), a linear increase in aromatic content (Figure 4m) and a non-linear increase in protein with temperature (Figure 4i). *Chamaedaphne* fatty acid content declined significantly with temperature (Figure 4d). The full coefficient table for this model is provided in the Supplement (Supplemental Table S3).

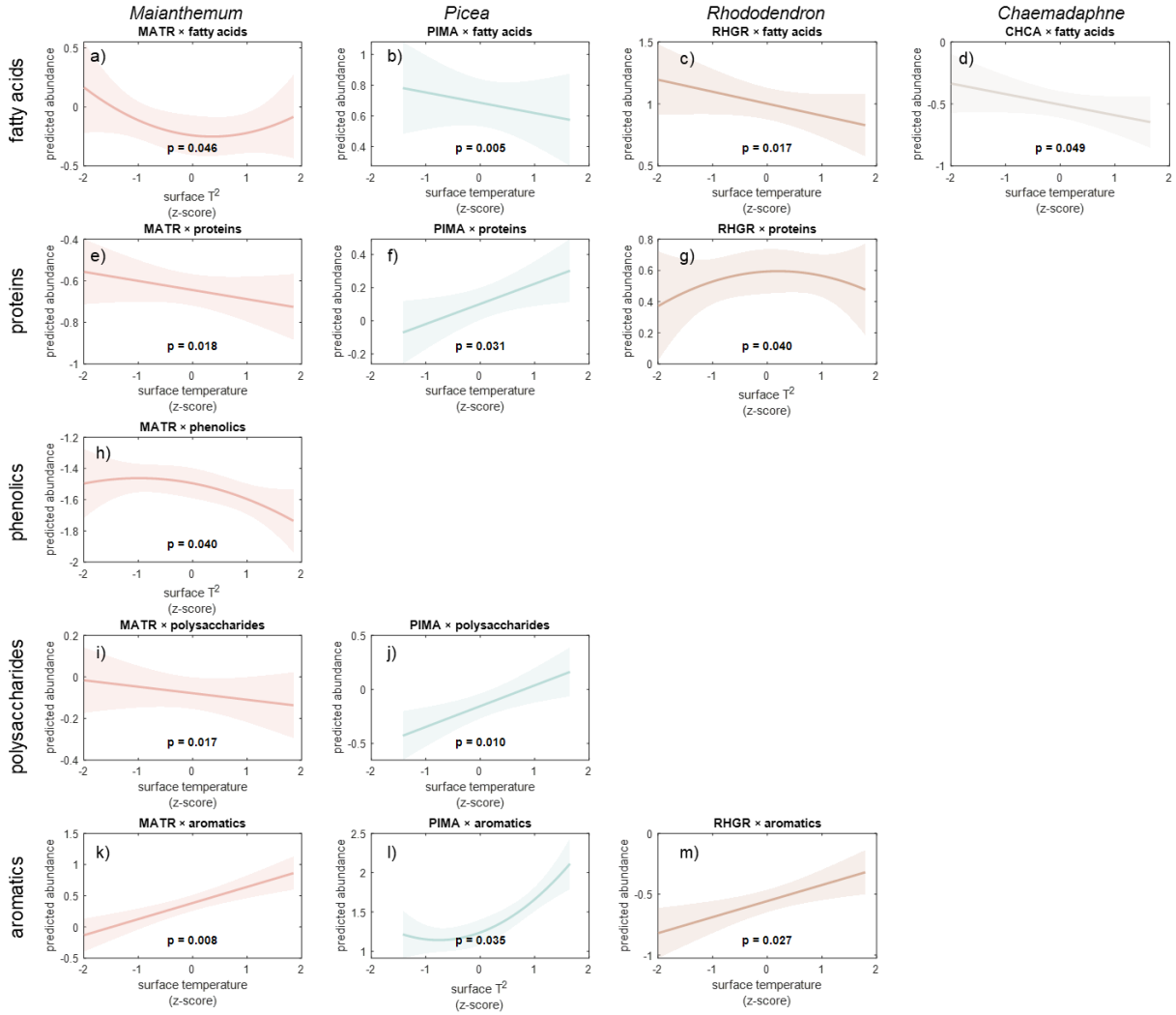

Figure 4: Significant predicted plant chemical linear and non-linear temperature responses (from fitlme model), species with non-significant trends are not shown. P-values for the temperature response are given in each panel which plots the response and 95% confidence interval as the shaded area. Plots are arranged into columns by Species and into rows by chemical classes.

The response of changing plant chemical inputs to the surface under different temperatures (under ambient and eCO_2) is shown in the Supplement (Figure S3). Under ambient conditions polysaccharides increase with temperature but not significantly (t-stat = 1.9, df = 672, p = 0.05), but under eCO_2 the temperature response is negative and significant (t-stat = -4.4, df = 672, p = 1e-5). Glycosides do not response to temperature under either ambient or elevated CO_2. Phenolics (t-stat = 2.1, df = 672, p = 0.03) decline under ambient CO_2, but switch to positive under elevated CO_2 (t-stat = -3.8, df = 672, p = 1e-4). Lignin (t-stat = 3.6, df = 672, p = 3e-4) and protein-like (t-stat = 3.5, df = 672, p = 5e-4) compounds increase under ambient CO_2 and decline with temperature under elevated CO_2 treatment (t-stat = -5.2, df = 672, p = 1.9e-7 and t-stat = -5.4, df = 672, p = 9e-8 respectively).

3.2 Porewater Phenolics and FTICR-MS-based Metabolomics

The porewater chemical composition changed significantly with temperature (main effect t-stat = 2.83; df = 3932; $p < 0.001$) under both ambient and elevated CO_2 treatment (Figure 5). Although no main effect of CO_2 treatment was observed ($p > 0.1$), interaction with temperature were observed such that CO_2 treatment alters the temperature response ($eCO_2 \times T$, t-stat = -3.6; df = 3932; $p = 0.0003$). In some cases, the eCO_2 treatment amplified the temperature response (e.g. proteins, condensed aromatics) and in some cases mitigated (e.g. phytochemicals) or even reversed the temperature response (e.g. phenolics, phospholipids, lignins). Depth did not have a significant main or interaction effect ($p > 0.1$ for both).

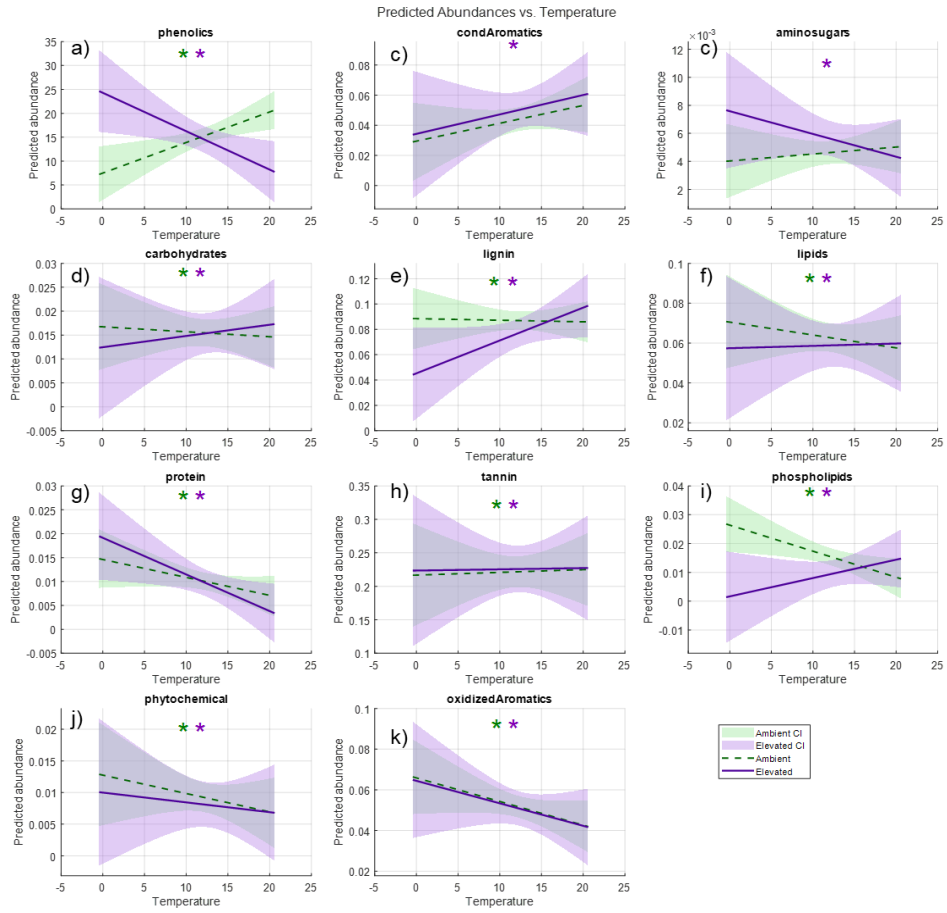

Figure 5: Predicted temperature response of the FTICR-MS determined compound classes in porewater vs soil temperature from the mixed effects modeling under ambient (green-dashed line) and eCO_2 (purple solid line) treatment. 95% confidence intervals are indicated by the shaded area surrounding each line. Asterisks in each panel indicate whether the response is significant ($p < 0.05$) under ambient (green) or if the temperature response under eCO2 differs from the ambient response (purple asterisk). There was no main or interacting effect of depth in the model. The top image (credit R.M. Wilson) shows a representative piezometer nest in one of the enclosures.

3.3 Porewater CO_2 and CH_4

Depth and CO_2 treatment had significant main effects on porewater CO_2 content (Table 1). Although temperature alone did not have a significant main effect on porewater CO_2, its influence depended on the combined effects of depth and elevated atmospheric CO_2, indicating a significant three-way interaction ($t = 3.3$, $df = 158$, $p = 0.03$). At elevated CO_2 treatment, warming has a stronger positive effect on porewater CO_2 at depth compared to ambient CO_2 conditions. The chemicals in the porewater that were significant predictors of porewater CO_2 were aminosugars (positive, t-stat = 3.3, df = 158, p = 0.001), lignin (positive, t-stat = 1.99, df = 158, p = 0.048) and phospholipids (negative, t-stat = -2.78, df = 158, p = 0.01).

There was not a main effect of temperature on porewater CH_4 concentrations, but there was an interaction with depth such that the temperature response declines with depth (t-state = -2.49, df = 153, p = 0.01). Phenolics (t-stat = -2.1, df = 153, p = 0.03) and phospholipids (t-stat = -2.67, df = 153, p 0.01) were negative predictors of CH_4 in the porewater. In contrast, aminosugars (t-stat = 2.19, df = 153, p = 0.03) and lignin (t-stat = 2.5, df = 153, p = 0.01) were positive predictors of CH_4 in the porewater (Table 1).

Alpha is a metric derived from the isotope difference between the CO_2 and CH_4 ($[\delta^{13}CO_2 + 1000]/[\delta^{13}CH_4 + 1000]$) that can be used as indicator of the relative strength of the two dominant methanogenesis pathways in the peat. High alpha (~1.045 to 1.09) indicates hydrogenotrophic methanogenesis, while low alpha (<1.045) indicates greater acetoclastic methanogenesis (Whiticar 1999). There is an overall significant negative response of alpha to temperature (t-stat = -2.8, df = 154, p = 0.01) indicating more acetoclastic CH_4 production. The temperature response of alpha increases with depth (t-stat = 4.57, df = 154, p < 0.001). There is no significant main or interaction effect of eCO_2 treatment on alpha (Table 1).

Table 1: Mixed Effects Modeling for C gas dynamics. Main and interaction effects of temperature (T), depth, and eCO_2 treatment were tested as well as porewater chemical composition as predictors.

Response	Predictor	· estimate	SE	t-stat	DF	p-value
CO_2	depth	0.63	0.11	5.5	158	1.3e-7
	eCO_2	0.56	0.19	3.0	158	2.8e-3
	eCO_2 × depth	-0.3	0.14	-2.1	158	0.04
	eCO_2 × T × depth	0.27	0.12	2.3	158	0.03
	amino sugars	0.47	0.14	3.3	158	1.2e-3
	lignin	0.28	0.14	2.0	158	0.048
	phospholipids	-0.44	0.16	-2.8	158	0.01
CH_4	T × depth	-0.21	0.08	-2.5	153	0.01
	phenolics	-0.25	0.12	-2.1	153	0.03
	amino sugars	0.34	0.16	2.2	153	0.03
	lignin	0.38	0.15	2.5	153	0.01
	phospholipids	-0.46	0.17	-2.7	153	0.01
alpha	T	-0.28	0.10	-2.78	154	6e-3
	depth	0.31	0.08	4.1	154	5.8e-5
	T × depth	0.22	0.05	4.57	154	9e-6
	lignin	0.27	0.10	2.57	154	0.01

Using a network approach, we combined the results of the mixed effects model in a nested hierarchy to evaluate the indirect and direct effects of biomass-weighted plant chemical inputs first on

porewater chemical composition and then overall C gas production dynamics as measured by CO_2 and CH_4 concentrations and alpha (Figure 6). In these networks we show only positive effects of plant inputs on porewater chemistry (in keeping with our hypothesis), while both positive and negative effects of porewater chemistry on C gas measures are considered. We found that plant polysaccharide input has a strong effect on porewater aminosugar content which in turn drives both CO_2 and CH_4 concentrations in a positive fashion (Figure 6). Plant lignin inputs are positively (though not significantly) correlated with pore water lignin, and significantly correlated with porewater phenolic content which in turn suppresses CH_4 while having no apparent effect on porewater CO_2 concentrations. Phospholipids in the porewater have an inhibitory effect on both CO_2 and CH_4 concentrations, but do not appear to be influenced by plant inputs. Alpha is significantly predicted only by plant lignin inputs.

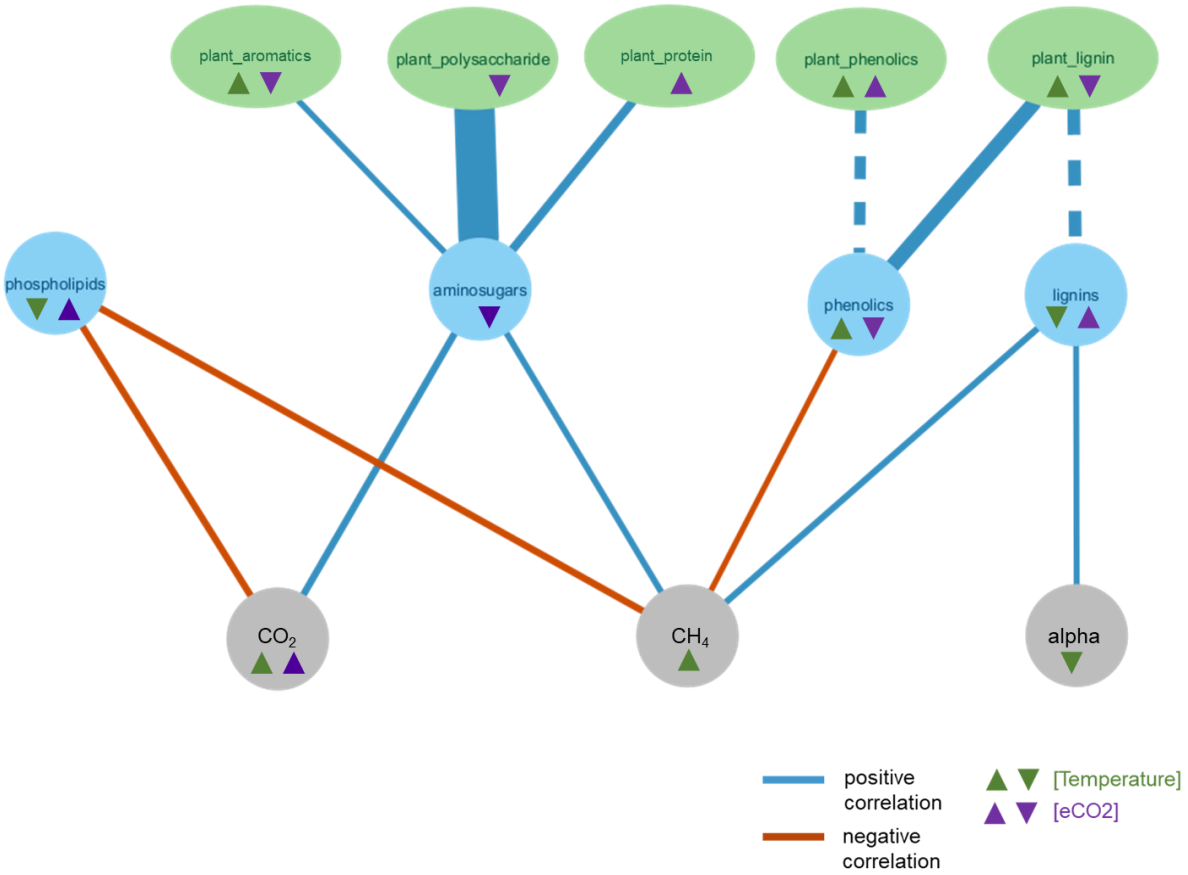

Figure 6: Network illustrating direct and indirect effects of plant chemical inputs on porewater chemical composition and in turn the porewater chemical composition on C gas production dynamics. Blue lines indicate positive correlations between nodes; red lines indicate negative correlations between nodes as determined from the nested mixed effects modeling. The magnitude of the correlation is indicated by the thickness of the line, thicker lines indicate a larger ･ . Solid lines indicate significant effects ($p < 0.05$), dashed lines indicate strong correlations (･ > 1) with marginal significance ($p < 0.1$). Green triangles indicate temperature responses under ambient CO_2 treatment, upward pointing triangle indicate positive

temperature correlation downward point triangle indicate negative correlation. Purple triangles similarly indicate the direction of the temperature responses under elevated CO_2 treatment.

3.4 Microbial community composition results

Differential abundance analysis of the porewater microbial communities identified 20 unique genera that increased significantly between the +0ºC and +9ºC treatments ($p < 0.05$; Figure 7a). The majority of these taxa showed a significant increase in relative abundance with warming at the mid-range depths, including 13 and 7 genera at 50 cm and 75 cm depth, respectively. Several genera were found to respond to warming across multiple depths, including *Candidatus* Methylopumilus, *Pedobacter*, *Rhodoferax*, and *Crenothrix*.

Of the 20 microbial groups that increased with warming, 4 of these groups were also found to significantly differ between the ambient and elevated CO_2 treatments (Wilcoxon test, $p < 0.05$; Figure 7b). These included the *Crenothrix*, *Methylomonas*, *Candidatus* Zambryskibacteria, and Methylomonadaceae. Interestingly, these taxa only differed between CO_2 treatments in the +9ºC enclosures at 25cm depth, with no significant changes detected in the +0ºC enclosures.

To identify shifts in microbial community composition with geochemical measurements, we performed linear regressions of the 20 taxa that responded to warming against CO_2:CH_4 ratios measured from the corresponding depths and enclosures. This analysis revealed 9 taxa whose relative abundances were significantly higher at low CO_2:CH_4 ratios (i.e., under more methanogenic conditions; $p < 0.05$; Figure 7c).

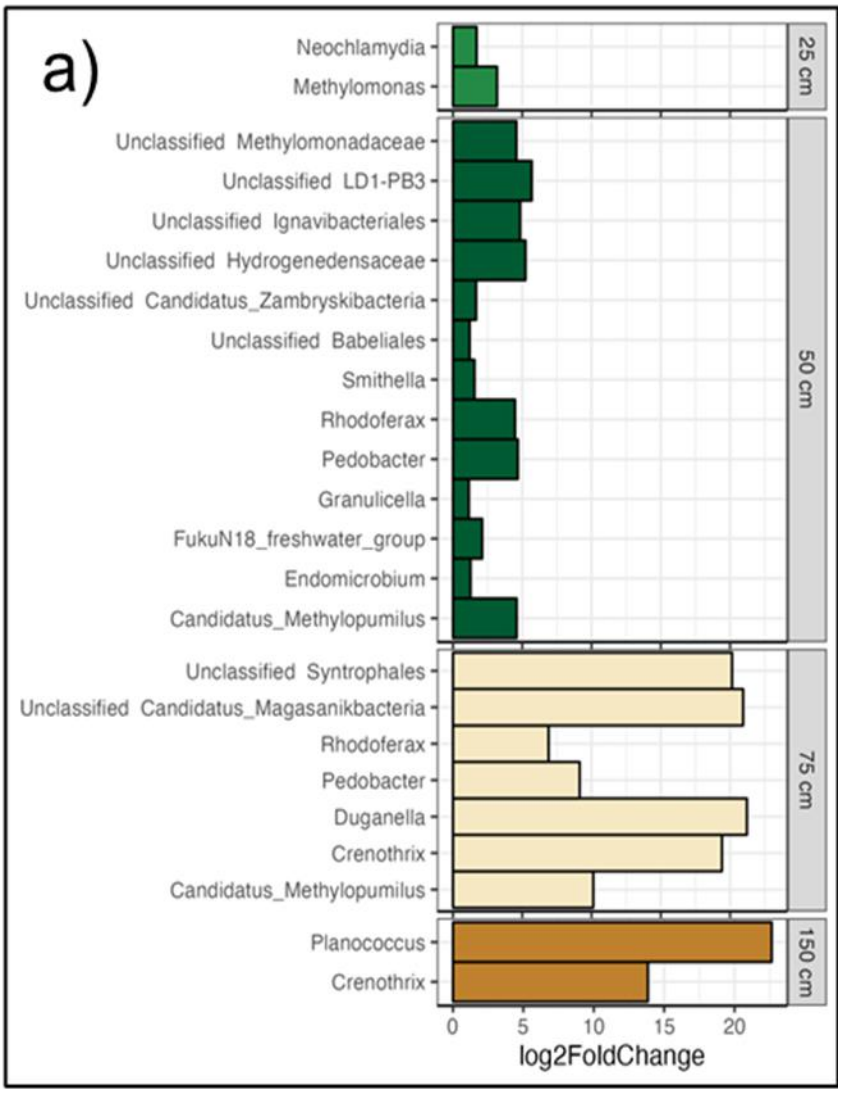
a)
Neochlamydia
Methylomonas
Unclassified Methylomonadaceae
Unclassified LD1-PB3
Unclassified Ignavibacteriales
Unclassified Hydrogenedensaceae
Unclassified Candidatus_Zambryskibacteria
Unclassified Babeliales
Smithella
Rhodoferax
Pedobacter
Granulicella
FukuN18_freshwater_group
Endomicrobium
Candidatus_Methylopumilus
Unclassified Syntrophales
Unclassified Candidatus_Magasanikbacteria
Rhodoferax
Pedobacter
Duganella
Crenothrix
Candidatus_Methylopumilus
Planococcus
Crenothrix
25 cm
50 cm
75 cm
150 cm
0
5
10
15
20
log2FoldChange

493

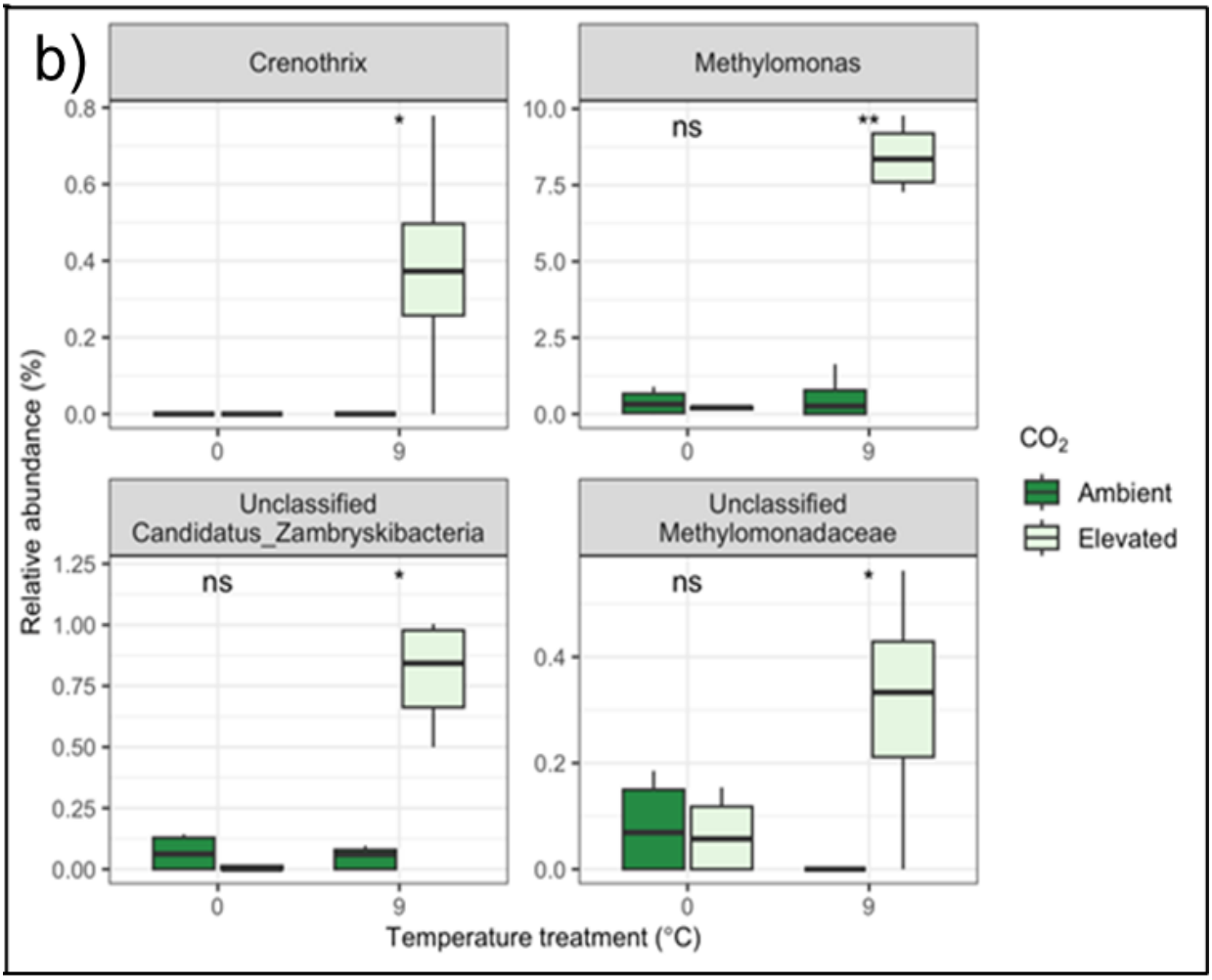
b)
Crenothrix
Methylomonas
Unclassified Candidatus_Zambryskibacteria
Unclassified Methylomonadaceae
Relative abundance (%)
Temperature treatment (°C)
ns
*
**
CO2
Ambient
Elevated

494

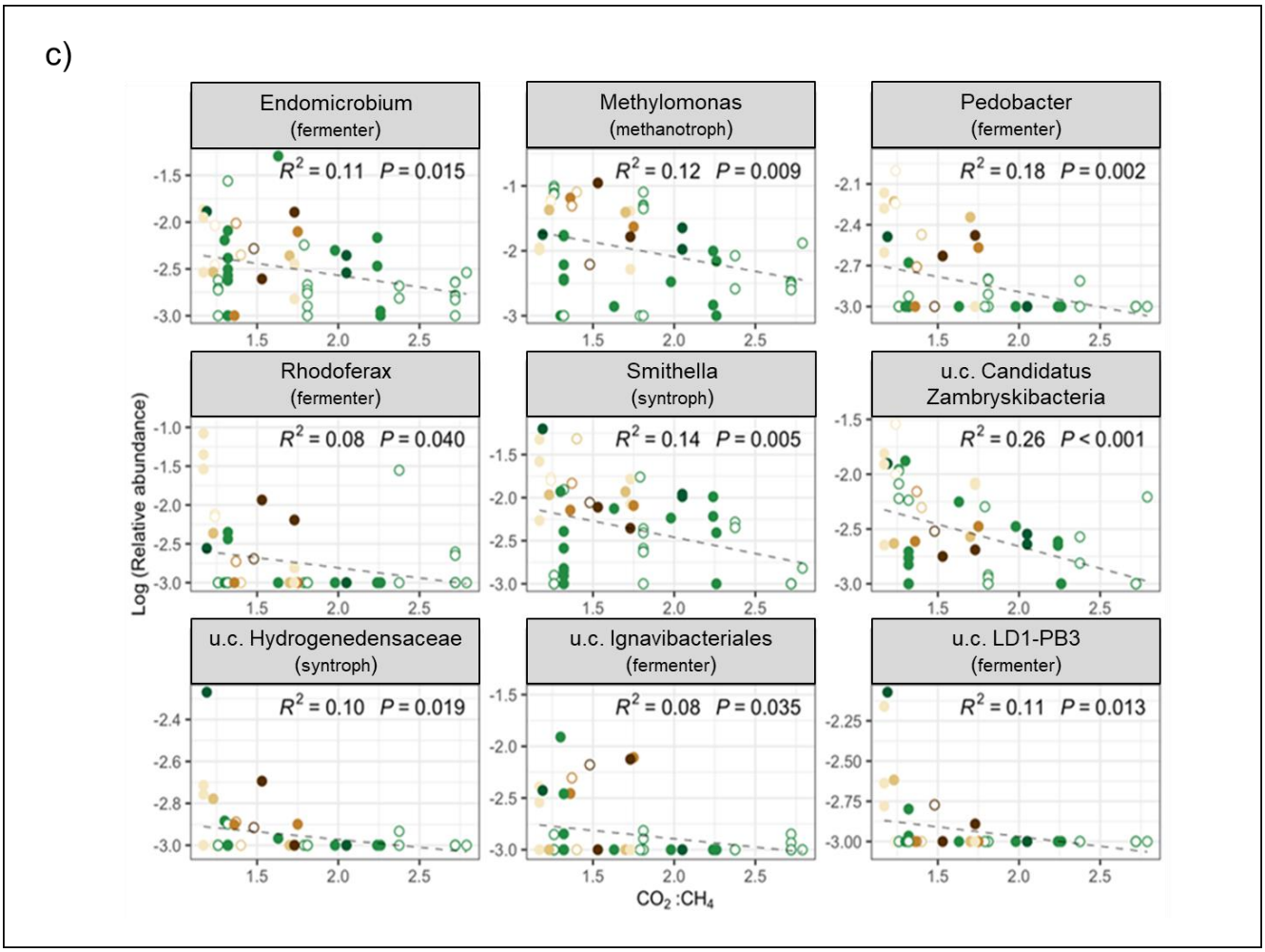

Figure 7: Panel (a) Porewater microbial taxa that increase with warming treatments. Responses to warming were determined using differential abundance analysis (DESeq2) to identify genus-level taxa that increased significantly between the +0ºC and +9ºC treatments ($p < 0.05$). Genera are separated according to their depth of origin in the porewater. Depths that are not shown did not contain any taxa with significant responses to warming treatments. The x-axis shows the magnitude of increase in relative abundance with warming, presented as the log2-fold change. Panel (b) Porewater microbial taxa impacted by warming and elevated CO_2 treatments at 25 cm depth. Prior to analysis, all amplicon sequence variants (ASVs) were merged at the genus-level. Boxplots represent genus-level taxa from replicate samples (n=3) as well as the two sampling time points (June 2016 and August 2017). Asterisks indicate the significance level for differences between the two CO_2 treatments at each temperature using a Wilcoxon test (* $p<0.05$; ** $p<0.01$), ns indicates a non-significant difference ($p>0.05$). Panel (c) Regressions of porewater microbial taxa abundances against CO_2:CH_4 ratios. Regressions were performed for all 20 microbial genera that responded positively to warming treatments using differential abundance analysis. Here, only those taxa with significant correlations to CO_2:CH_4 ratios are shown ($p < 0.05$). Porewater depths are represented by color as in Figure 5, while CO_2 treatments are indicated by open vs. closed points. Relative abundance values were log-transformed to meet expectations of normality. Unclassified taxa are indicated as "u.c.".

4 Discussion

4.1 Plant community changes with warming

In this ombrotrophic bog, whole ecosystem warming altered the dominant plant community including a dramatic decline in *Sphagnum* species accompanied by a substantial increase in shrubs (*Rhododendron* and in 2021 *Chamaedaphne* see supplemental Table S2) (Figure 2; Norby et al., 2019; McPartland et al., 2020). As in other peatlands (Wilson et al., 2022), plant species exhibited distinct chemical compositions (Figure 3). In addition to differences in chemical composition among plant species, chemical composition within species changed in response to warming (Figure 4). We hypothesized that changes in plant community and plant chemical composition in response to the warming treatments were likely to change the quality or organic inputs to the subsurface which would then influence C gas production dynamics. As plants are the primary source of organic matter to the subsurface in ombrotrophic peatlands, they play a strong role in controlling the availability of organic substrates fueling heterotrophic microbial processes (Sutton-Grier and Megonigal 2011) that result in organic matter decomposition to the greenhouse gases CO_2 and CH_4. We hypothesized that changes in the abundance of plant-associated compounds could be used to predict changes in CO_2 and CH_4 production dynamics (Figure 1).

At this same boreal bog site, McPartland et al., (2020) found that the relative cover of *Sphagnum* moss and the forb *Maianthemum* significantly declined with warming, while the shrub *Vaccinium angustifolium* increased. They found contradictory results for aboveground biomass of *Rhododendron groenlandicum* during the early stages of the experiment, but after extending the dataset to 2022, both *R. groenlandicum* (overall years, Figure 2) and *Chamaedaphne calyculata* (in 2021 Table S2) increased with warming. Initially, there was no effect of warming on trees, however after almost eight years of treatment, the aboveground biomass of trees has increased with temperature as have shrubs. These increases come at the expense of *Sphagnum* (Hanson et al., 2025, Norby et al., 2019; 2023). While warming continues to cause substantial shifts to the increasingly shrub-dominated vegetation (Norby et al., 2019; McPartland et al., 2020), the effects of elevated CO_2 on the plant community in the early years of the experiment appear to be minimal (McPartland et al., 2020). However, more recently, Hanson et al., (2025) have observed the emergence of an eCO_2 response, wherein shrub biomass is higher in the elevated air CO_2 plots. This lag was attributed to the nutrient poor conditions within this ombrotrophic bog (Hanson et al., 2025). In the early years of the experiment, production was nutrient limited, but as the *Sphagnum* died off and released organic material to the subsurface via decomposition the nutrient limitation was hypothesized to be alleviated (Iversen et al., 2023) allowing the trees and shrubs to respond to the elevated CO_2 (Hanson et al., 2025).

4.2 Differences in plant chemical composition and changes with warming

The observed vegetation changes have resulted in changing plant chemical inputs to the subsurface. As the plant community composition shifts from *Sphagnum*-dominated, with high polysaccharide content, towards shrubs, with higher phenolic and aromatics content, the resulting potential inputs of bioavailable organic inputs changes. *Sphagnum*, of course, does not contain true lignin, so the shift towards trees and shrubs does, by default, increase lignin inputs. This is reflected in the higher lignin-like compounds in *Picea* and *Vaccinium* (Figure 3f). The lignin-like FTIR band at 1515 is also associated with pectin (Synytsya et al., 2003) which is present in *Sphagnum* cell walls (Ballance et al., 2012), hence our description of this band as lignin-like. The relatively lower phenolic content of *Sphagnum* compared to the trees and shrubs we observe here (Figure 3d) is consistent with other studies demonstrating increasing phenolic content in trees and shrubs during peatland vegetation shifts (Bragazza et al., 2012; Wang et al., 2015). This increasing phenolic content is thought to (1) be somewhat resistant to microbial decomposition itself, although some utilization occurs (McGivern et al., 2024) and (2) protect the *Sphagnum* peat that is there from being readily degraded (Wang et al., 2015).

In addition to changes in plant inputs due to changing species composition, there are also shifts in the molecular composition within individual plant species, some of which mitigate the shifts in plant species. *Picea* exhibits increasing polysaccharide content with temperature consistent with observations that some plants, including pines, increase polysaccharide content in response to drought stress in order to improve osmoregulation (Chandrasekaran et al., 2022). Aromatic contents increased in *Maianthemum*, *Picea*, and *Rhododendron* in response to temperature, consistent with observations of increasing aromatic content (such as aromatic amino acids) in the model species Arabidopsis (Kaplan et al., 2004). Increasing protein content in *Picea* and *Rhododendron* is consistent with the production of heat shock proteins in these longer-lived species (Spinelli et al., 2011).

Because the model did not converge with the full four-way interaction, we could not assess eCO_2 effects within individual plant species. Instead, we evaluated the combined effects of temperature and eCO_2 on biomass-weighted inputs of plant organic matter to the soil. Collectively, increased shrub and tree abundance, along with changes in plant chemical composition, led to a net decline in the inputs of highly bioavailable compounds (e.g., polysaccharides) and an increase in less bioavailable compounds (e.g., lignin) with warming under ambient CO_2 conditions (Supplemental Figure 3). This decline in bioavailable organic matter with warming is consistent with global shifts in peat composition reported by Verbeke et al (2022) and Hodgkins et al. (2018).

4.3 Correlations of plant chemical composition with porewater organic matter availability

Shifts in plant inputs appear to strongly influence porewater chemistry, in particular, compounds linked to C gas production. Highly bioavailable inputs, such as plant polysaccharides were closely associated with higher porewater aminosugar content, with smaller contributions from plant proteins and non-lignin aromatics. This pattern is consistent with the fermentation of cell wall polysaccharides into constituent monomers, including aminosugars (Hu et al., 2018). The breakdown of polysaccharides is often considered the rate-limiting step for fermentation, particularly in environments like peatlands which are highly N-limited (Hu et al., 2018). In *Sphagnum*-dominated peatlands, where fermentation products tend to accumulate (Zalman et al., 2018, Tveit et al., 2015), greater aminosugar release under warming may therefore stimulate microbial metabolism by increasing N availability, ultimately promoting CO_2 and CH_4 production. Aminosugar content could be driven by leaching from dead *Sphagnum* biomass into the belowground pool an explanation consistent with earlier data showing the transfer of nitrogen compounds from *Sphagnum* decomposition into belowground pools (Petro et al., 2023). Further, porewater aminosugars and carbohydrates (under eCO_2) may result from overall increases in aboveground net primary production (McPartland et al., 2020) rather than changes in individual plant species or community composition and their chemistry. The decline in porewater protein concentration with increasing temperature under both ambient and eCO_2 (Figure 5g) is consistent with earlier observed trends and supports the hypothesis that microbial protein uptake increases with warming due to higher turnover rates (Wilson et al., 2021a). The absence of a clear relationship between plant protein inputs (Figure S3) and porewater protein levels could therefore reflect rapid microbial recycling of these compounds. In addition, enhanced protein degradation with warming could release N-rich aminosugars in the porewater explaining the positive correlation between plant protein inputs and porewater aminosugar content (Figure 6).

In contrast with earlier years of the experiment (Wilson et al., 2021a), the extended time series no longer shows a significant increase in carbohydrate-like compounds in the porewater with warming (under ambient CO_2 conditions; Figure 5d). In the short-term, warming stimulates sugar production within plants in response to abiotic stress (Chandrasekaran et al., 2022)— a pattern consistent with our observations of increasing polysaccharide content in trees (Figure 4j). However, the longer term shifts in plant community composition, specifically the overall loss of polysaccharide-rich *Sphagnum* (Figure 3d), offset these short-term increases at the individual plants level and result in a net decline of polysaccharide inputs to the subsurface over time.

The strong correlation between plant lignins and porewater phenolics— even more so than with porewater lignin content— suggests that these are primarily hydrolysable lignin that are rapidly degraded to their phenolic subunits. Interestingly, porewater phenolic content suppressed CH_4 production, but did not influence CO_2 production (Figure 6). It is thought that phenolic compounds may uniquely inhibit

methanogens within the microbial community, a phenomenon that has been shown to occur in laboratory incubations (McGivern et al., 2024, 2025), and that we now demonstrate here in the field. Phospholipids were not significantly predicted by any plant inputs and appear to be microbially driven.

The changing plant organic matter inputs to the subsurface are reflected in the changing microbial community, particularly lineages (e.g. *Pedobacter, Granulicella*, and Ignavibacteriales) that have been linked to the breakdown and utilization of complex plant-derived polysaccharides (Pankratov and Dedysh, 2010; Podosokorskaya et al., 2013; Rawat et al., 2014; Wilkins et al., 2014). *Pedobacter* and Ignavibacteriales may also function as primary fermenters of simple sugars such as glucose, allowing them to utilize the products of their own hydrolytic activities (Podosokorskaya et al., 2013; Wilkins et al., 2014; Bei et al., 2021). Other primary fermenters responding to warming include members of *Endomicrobium* (Figures 7a, c) (Stingl et al., 2005) which grow by fermenting glucose to lactate, acetate, hydrogen, and CO_2 (Hongoh et al., 2008; Zheng et al., 2016) all precursors to CO_2 and CH_4 production.

In agreement with our previous work (Hopple et al., 2020; Wilson et al., 2021a), the abundance of methanogens did not change with warming. This suggests that enhanced decomposition and substrate availability stimulates methanogen activity, but not their growth. This might be because methanogens grow very slowly under the harsh conditions (cold, acidic, low N) found in the peat subsurface and the amount of warming in this experiment is insufficient to overcome those constraints.

4.3 *Dynamics in porewater CO_2 and CH_4 with temperature*

Since whole ecosystem warming was initiated at the site, porewater CO_2 concentrations have risen with temperature (Wilson et al., 2021a). In our model only the 3-way interaction between temperature × depth × eCO_2 was significant indicating that the temperature response of CO_2 production varies with depth and depends highly on the eCO_2 treatment (Table 1). In the elevated CO_2 treatments, higher porewater CO_2 reflects overall higher biomass from primary production boosts (McPartland et al., 2020). Earlier in the experiment (prior to 2020), porewater CH_4 concentrations were significantly correlated with temperature only at the surface (10 – 25 cm) (Wilson et al., 2021a). Our extended analysis shows that the temperature response of CH_4 is attenuated by depth, but is not influenced by the eCO_2 treatment (Table 1). The overall increase in CH_4 production under warming is likely influenced by a combination of ecosystem-level processes. For example, warming can increase methane production by stimulating overall microbial activity. However, warming also shifts plant inputs toward less bioavailable substrates. At the same time, higher evapotranspiration under warmer conditions can lower the water-table (Girardin et al., 2016) which increases O_2 infiltration into the subsurface, further constraining methanogenesis, which is a strictly anaerobic process.

Alpha, a measure of the isotopic difference between the two microbial respiration products CO_2 and CH_4, serves as a proxy for the dominant pathways of methanogenesis. In contrast with our previous work (e.g., Wilson et al., 2021a), our extended data now reveals a consistent shift towards acetoclastic methanogenesis as the peat warms. Given that hydrogenotrophic methanogenesis is thought to be more sensitive to warming than acetoclasty (Dellagnezze et al., 2023), it seems likely that the shift in pathways observed here is due to changing substrate inputs rather than a direct result of warming. For example, the decrease in lignin-like compounds and the positive correlation between porewater lignin-like content and increasing alpha (Table 1)— i.e. more hydrogenotrophic methanogenesis— is consistent with the prediction that more bioavailable organic matter favors acetoclastic over hydrogenotrophic CH_4 production (Chanton et al., 2008; Tveit et al., 2015 Conrad 1999; D'Andrilli et al., 2010). Together with the increase in overall CH_4 production, these results cumulatively point to a priming effect whereby an enhancement in plant-derived organic matter inputs with warming at the surface are stimulating overall decomposition at deeper peat depths, a result that is consistent with radiocarbon analyses from the site (Wilson et al., 2021b).

4.4 Linkages between microbial community dynamics and pathways of organic matter decomposition

Shifts in the porewater microbial community are consistent with our hypothesis that warming stimulates terminal decomposition through methanogenesis. Numerous heterotrophic taxa, including known syntrophs (e.g. *Syntrophales*) which produce both acetate and H_2 (Conrad 1999), increased in relative abundance with warming. They were most concentrated at intermediate depths (50-75cm) coinciding with the decline in alpha and the increase in CH_4 concentrations with increasing temperature (Table 1) highlighting this depth as particularly sensitive to warming (e.g. Tfaily et al., 2018). Many of the taxa that are more abundant in the warmer treatments are also associated with more methanogenic conditions in the porewater. Among them, *Smithella* (de Bok et al., 2001; Schmidt et al., 2016; Wang et al., 2019) and the uncultivated family-level lineage Hydrogenedentes (Nobu et al., 2015), are syntrophs that partner with methanogens to further decompose primary fermentation products.

The co-occurrence of hydrolytic, fermentative, and syntrophic microorganisms with lower CO_2:CH_4 (i.e., more methanogenic conditions) and elevated concentrations of the byproducts of plant-derived lignin degradation (i.e. phenolics Figures 5a and 6) suggests that warming is stimulating methane production via increased organic matter decomposition and the upstream supply of methanogenic substrates. Accumulation of methanogenic substrates can be linked to the increase in productivity for vascular plants in the warmed enclosures, resulting in inputs of fresh organic matter as plant litter and root exudates (Malhotra et al., 2020; McPartland et al., 2020; Wilson et al., 2021a). Elevated supply of plant-derived organic matter accelerates decomposition (Keuper et al., 2020; Ofiti et al., 2023) and here, we see

that changes in the microbial community composition toward a functional network of organic matter decomposing microorganisms increases organic matter cycling and higher rates of methanogenesis.

Consistent with Petro et al., (2023), warming also stimulated methanotrophs, including members of the genus *Methylomonas,* which increased with warming at the surface (25 cm; Figure 7) and was associated with lower CO_2:CH_4 ratios across the depth profile (Figure 7c). Members of *Methylomonas* are abundant and highly active in boreal peatlands (Kip et al., 2011; Esson et al., 2016), capable of oxidizing both CH_4 and methanol in culture (Ogiso et al., 2012; Danilova et al., 2013) and may play an important role in methylotrophic methanogenesis, which was previously highlighted as an overlooked but potentially important pathway in this peatland (i.e. Wilson et al., 2021a; Zalman et al., 2018). Below 25 cm, methanotrophs and methylotrophs, including *Candidatus* Methylopumilus (50 & 75 cm depth), a methanol user (Salcher et al., 2015) and *Crenothrix* (75 & 150 cm depths) increased with warming. Members of the *Crenothrix* group are unique in that they can oxidize methane both aerobically and anaerobically (Stoecker et al., 2006; Oswald et al., 2017), which may explain their presence in consistently anoxic peat. Interestingly, many of these taxa increased in abundance under the warming plus elevated CO_2 enclosures relative to the warming only treatments (25 cm; Figure 7b), suggesting that warming and CO_2 enrichment may have interactive impacts on CH_4 oxidation.

5 Conclusions

The plant community response to warming in our peatland WEW experiment reveals complex mechanisms linking vegetation change to C gas production. Our findings demonstrate that warming alters organic matter inputs through two distinct pathways: shifts in plant community composition and changes in molecular composition within individual plant species. The combined effect of these changes manifest in the subsurface dissolved organic matter pool, where we observed increased availability of N-containing aminosugars that correlate with enhanced CH_4 production. Critically, this enhanced methanogenesis appears driven by both direct temperature effects and indirect effects through changing plant inputs. The observed shift toward acetoclastic methanogenesis at higher temperatures, coupled with increasing porewater phenolics, suggests a fundamental change in carbon processing pathways. Our integration of plant chemistry, porewater metabolomics, and microbial community analysis reveals that ecosystem responses to warming may be cryptic and extend beyond visible vegetation changes. The complex interactions between plant inputs, microbial metabolism, and greenhouse gas production highlight the need for comprehensive monitoring approaches that capture both above and belowground responses to climate change. These findings have important implications for predicting and modeling peatland carbon cycling under future climate scenarios.

Acknowledgments

All authors declare there is no financial conflict of interest. This study was funded by the US Department of Energy (DOE), Office of Biological and Environmental Research, Terrestrial Ecosystem Science Program, under US Department of Energy (DOE) Contracts DE-SC0023297, DE-SC0007144 and DE SC0012088. The Oak Ridge National Laboratory is managed by UT-Battelle, LLC, for the US DOE under Contract DE-AC05-00OR22725. A portion of this research was performed using Environmental Molecular Sciences Laboratory (EMSL) (grid.436923.9) (proposal: Wilson ID 49279), a DOE Office of Science User Facility sponsored by the Office of Biological and Environmental Research and located at the Pacific Northwest National Laboratory (PNNL). The PNNL is a multiprogram national laboratory operated by Battelle for the DOE under Contract DE-AC05-76RLO 1830. The participation of R.K.K. and S.D.S. was funded by the Northern Research Station of the USDA Forest Service. The United States Government and the publisher, by accepting the article for publication, acknowledge that the United States Government retains a nonexclusive, paid-up, irrevocable, worldwide license to publish or reproduce the published form of this manuscript, or
allow others to do so, for United States Government purposes. The DOE will provide public access to these results of federally sponsored research in accordance with the DOE Public Access Plan (http://energy.gov/downloads/doepublic-access-plan).

Open Research

All data presented in this manuscript are publicly available. Metabolomics and gas data are publicly available from the SPRUCE long-term repository (doi: https://doi.org/10.25581/spruce.083/1647173). All raw 16S rRNA sequences have been uploaded to NCBI under Bioprojects: PRJNA640652; PRJNA638786; PRJNA638601. Metagenomes are publicly available in the Joint Genome Institute (JGI) Genome Portal and NCBI Sequence Read Archive (SRA).

References

Artz, R. R., Chapman, S. J., Robertson, A. J., Potts, J. M., Laggoun-Défarge, F., Gogo, S., ... & Francez, A. J. (2008). FTIR spectroscopy can be used as a screening tool for organic matter quality in regenerating cutover peatlands. *Soil Biology and Biochemistry*, *40*(2), 515-527.

Bailey, V. L., Smith, A. P., Tfaily, M., Fansler, S. J., & Bond-Lamberty, B. (2017). Differences in soluble organic carbon chemistry in pore waters sampled from different pore size domains. Soil Biology and Biochemistry, 107, 133-143.

749 Ballance, S., Kristiansen, K. A., Skogaker, N. T., Tvedt, K. E., & Christensen, B. E. (2012). The
750 localisation of pectin in Sphagnum moss leaves and its role in preservation. *Carbohydrate*
751 *polymers*, *87*(2), 1326-1332.
752
753 Bancuta O, Chilian A, Bancuta I, Ion RM, Setnescu R, Setnescu T et al. (2016). Improvement of
754 spectrophotometric method for determination of phenolic compounds by statistical investigations.
755 Romanian Journal of Physics, 61, 1255-64.
756
757 Bei, Q., Peng, J., & Liesack, W. (2021). Shedding light on the functional role of the Ignavibacteria in
758 Italian rice field soil: A meta-genomic/transcriptomic analysis. Soil Biology and Biochemistry,
759 163, 108444.
760
761 Bragazza, L., Parisod, J., Buttler, A. & Bardgett, R. D. (2012) Biogeochemical plant–soil microbe
762 feedback in response to climate warming in peatlands. Nature Clim. Change 3, 273–277.
763
764 Breitling, R., Ritchie, S., Goodenowe, D., Stewart, M. L., & Barrett, M. P. (2006). Ab initio prediction of
765 metabolic networks using fourier transform mass spectrometry data. Metabolomics, 2, 155–164.
766 https ://doi.org/10.1007/s11306-006-0029-z
767
768 Callahan, B. J., McMurdie, P. J., Rosen, M. J., Han, A. W., Johnson, A. J. A., & Holmes, S. P. (2016).
769 DADA2: High-resolution sample inference from Illumina amplicon data. Nature methods, 13(7),
770 581-583.
771
772 Caporaso, J. G., Lauber, C. L., Walters, W. A., Berg-Lyons, D., Lozupone, C. A., Turnbaugh, P. J., ... &
773 Knight, R. (2011). Global patterns of 16S rRNA diversity at a depth of millions of sequences per
774 sample. Proceedings of the national academy of sciences, 108(supplement_1), 4516-4522.
775
776 Chandrasekaran, U., Byeon, S., Kim, K., Kim, S. H., Park, C. O., Han, A. R., ... & Kim, H. S. (2022).
777 Short-term severe drought influences root volatile biosynthesis in eastern white pine (Pinus
778 strobus L). Frontiers in Plant Science, 13, 1030140.
779
780 Chanton, J. P., L. Chaser, P. Glaser, and D. Siegel (2005), Carbon and hydrogen isotopic effects in
781 microbial methane from terrestrial environments, in Stable Isotopes and Biosphere-Atmosphere

Interactions, edited by L. B. Flanagan, J. R. Ehleringer, and D. E. Pataki, pp. 85–105, Elsevier-Academic Press, San Diego, Calif.

Chanton, J.P., Glaser, P.H., Chasar, L.S., Burdige, D.J., Hines, M.E., Siegel, D.I., Tremblay, L.B. & Cooper, W.T. (2008). Radiocarbon evidence for the importance of surface vegetation on fermentation and methanogenesis in contrasting types of boreal peatlands. Global Biogeochemical Cycles, 22(4).

Cocozza, C., D'Orazio, V., Miano, T. M., & Shotyk, W. (2003). Characterization of solid and aqueous phases of a peat bog profile using molecular fluorescence spectroscopy, ESR and FT-IR, and comparison with physical properties. *Organic Geochemistry*, *34*(1), 49-60.

Conrad, R. (1999). Contribution of hydrogen to methane production and control of hydrogen concentrations in methanogenic soils and sediments. FEMS microbiology Ecology, 28(3), 193-202.

Corbett, J., Burdige, D. J., Glaser, P. H., & Chanton, J. (2012, December). Lab incubation experiments verify microbial respiration from recent photosynthetic production in deep peat within bog and fen environments. In AGU Fall Meeting Abstracts (Vol. 2012, pp. B21G-08).

Cory, A. B., Wilson, R. M., Holmes, M. E., Riley, W. J., Li, Y. F., Tfaily, M. M., ... & Chanton, J. P. (2025). A climatically significant abiotic mechanism driving carbon loss and nitrogen limitation in peat bogs. Scientific Reports, 15(1), 2560.

D'Andrilli, J., Chanton, J. P., Glaser, P. H., & Cooper, W. T. (2010). Characterization of dissolved organic matter in northern peatland soil porewaters by ultra high resolution mass spectrometry. Organic Geochemistry, 41(8), 791-799.

Danilova, O. V., Kulichevskaya, I. S., Rozova, O. N., Detkova, E. N., Bodelier, P. L., Trotsenko, Y. A., & Dedysh, S. N. (2013). Methylomonas paludis sp. nov., the first acid-tolerant member of the genus Methylomonas, from an acidic wetland. International journal of systematic and evolutionary microbiology, 63(Pt_6), 2282-2289.

de Bok, F. A., Stams, A. J., Dijkema, C., & Boone, D. R. (2001). Pathway of propionate oxidation by a syntrophic culture of Smithella propionica and Methanospirillum hungatei. Applied and environmental microbiology, 67(4), 1800-1804.

Dellagnezze, B. M., Bovio-Winkler, P., Lavergne, C., Menoni, D. A., Mosquillo, F., Cabrol, L., ... & Etchebehere, C. (2023). Acetoclastic archaea adaptation under increasing temperature in lake sediments and wetland soils from Alaska. Polar Biology, 46(4), 259-275.

Durak, T., & Depciuch, J. (2020). Effect of plant sample preparation and measuring methods on ATR-FTIR spectra results. *Environmental and Experimental Botany*, *169*, 103915.

Ellsworth, D. S., Thomas, R., Crous, K. Y., Palmroth, S., Ward, E., Maier, C., DeLucia, E., Oren, R. (2012) Elevated CO_2 affects photosynthetic responses in canopy pine and subcanopy deciduous trees over 10 years: a synthesis from Duke FACE. Global Change Biology 18(1), 223-242.

Esson, K. C., Lin, X., Kumaresan, D., Chanton, J. P., Murrell, J. C., & Kostka, J. E. (2016). Alpha-and gammaproteobacterial methanotrophs codominate the active methane-oxidizing communities in an acidic boreal peat bog. Applied and environmental microbiology, 82(8), 2363-2371.

Girardin, M. P., Hogg, E. H., Bernier, P. Y., Kurz, W. A., Guo, X. J., & Cyr, G. (2016). Negative impacts of high temperatures on growth of black spruce forests intensify with the anticipated climate warming. Global change biology, 22(2), 627-643.

Griffiths, Natalie A., et al. "Temporal and spatial variation in peatland carbon cycling and implications for interpreting responses of an ecosystem - scale warming experiment." *Soil Science Society of America Journal* 81.6 (2017): 1668-1688.

Hanson, P. J., Childs, K. W., Wullschleger, S. D., Riggs, J. S., Thomas, W. K., Todd, D. E., & Warren, J. M. (2011). A method for experimental heating of intact soil profiles for application to climate change experiments. Global Change Biology, 17(2), 1083-1096.

Hanson, P. J., Riggs, J. S., Nettles, W. R., Phillips, J. R., Krassovski, M. B., Hook, L. A., ... & Barbier, C. (2017). Attaining whole-ecosystem warming using air and deep-soil heating methods with an elevated CO 2 atmosphere. Biogeosciences, 14(4), 861-883.

Hanson, Paul J, Jana R Phillips, Stan D Wullschleger, W Robert Nettles, Jeffrey M Warren, Eric J Ward, Jake D Graham, and Thomas A Ruggles. 2018. SPRUCE Tree Growth Assessments of *Picea* and *Larix* in S1-Bog Plots and SPRUCE Experimental Plots beginning in 2011**.** Oak Ridge National Laboratory, TES SFA, U.S. Department of Energy, Oak Ridge, Tennessee, U.S.A. https://doi.org/10.25581/spruce.051/1433836

Hanson, P. J., Griffiths, N. A., Iversen, C. M., Norby, R. J., Sebestyen, S. D., Phillips, J. R., ... & Ricciuto, D. M. (2020). Rapid net carbon loss from a whole - ecosystem warmed Peatland. AGU Advances, 1(3), e2020AV000163.

Hanson, P. J., Griffiths, N. A., Salmon, V. G., Birkebak, J. M., Warren, J. M., Phillips, J. R., ... & Pearson, K. J. (2025). Peatland Plant Community Changes in Annual Production and Composition Through 8 Years of Warming Manipulations Under Ambient and Elevated CO2 Atmospheres. Journal of Geophysical Research: Biogeosciences, 130(2), e2024JG008511.

Hicks Pries, C. E., Schuur, E. A. G., Vogel, J. G., & Natali, S. M. (2013). Moisture drives surface decomposition in thawing tundra. Journal of Geophysical Research: Biogeosciences, 118(3), 1133-1143.

Hodgkins, S. B., Richardson, C. J., Dommain, R., Wang, H., Glaser, P. H., Verbeke, B., ... & Chanton, J. P. (2018). Tropical peatland carbon storage linked to global latitudinal trends in peat recalcitrance. Nature communications, 9(1), 1-13.

Hongoh, Y., Sharma, V. K., Prakash, T., Noda, S., Taylor, T. D., Kudo, T., ... & Ohkuma, M. (2008). Complete genome of the uncultured Termite Group 1 bacteria in a single host protist cell. Proceedings of the National Academy of Sciences, 105(14), 5555-5560.

Hopple, A. M., Wilson, R. M., Kolton, M., Zalman, C. A., Chanton, J. P., Kostka, J., ... & Bridgham, S. D. (2020). Massive peatland carbon banks vulnerable to rising temperatures. Nature communications, 11(1), 1-7.

Hough, M., McCabe, S., Vining, S. R., Pickering Pedersen, E., Wilson, R. M., Lawrence, et al. (2021). Coupling plant litter quantity to a novel metric for litter quality explains C storage changes in a thawing permafrost peatland. Global Change Biology.

Hu, Y., Zheng, Q., Zhang, S., Noll, L., & Wanek, W. (2018). Significant release and microbial utilization of amino sugars and D-amino acid enantiomers from microbial cell wall decomposition in soils. Soil Biology and Biochemistry, 123, 115-125.

Huang, Y., Ciais, P., Luo, Y., Zhu, D., Wang, Y., Qiu, C., Goll, D.S., Guenet, B., Makowski, D., De Graaf, I. and Leifeld, J., 2021. Tradeoff of CO_2 and CH_4 emissions from global peatlands under water-table drawdown. Nature Climate Change, 11(7), pp.618-622.

Hugelius, G., Loisel, J., Chadburn, S., Jackson, R. B., Jones, M., MacDonald, G., ... & Yu, Z. (2020). Large stocks of peatland carbon and nitrogen are vulnerable to permafrost thaw. Proceedings of the National Academy of Sciences, 117(34), 20438-20446.

Iversen CM, Garrett A, Martin A, Turetsky MR, Norby RJ, Childs J, Ontl TA. 2017. SPRUCE S1 Bog Tree Basal Area and Understory Community Composition Assessed in the Southern and Northern Ends of the S1 Bog. Carbon Dioxide Information Analysis Center, Oak Ridge National Laboratory, U.S. Department of Energy, Oak Ridge, Tennessee, U.S.A. http://dx.doi.org/10.3334/CDIAC/spruce.024

Iversen, C. M., Latimer, J., Brice, D. J., Childs, J., Vander Stel, H. M., Defrenne, C. E., ... & Hanson, P. J. (2023). Whole-ecosystem warming increases plant-available nitrogen and phosphorus in an ombrotrophic bog. Ecosystems, 26(1), 86-113.

Jones, M. C., Booth, R. K., Yu, Z., & Ferry, P. (2013). A 2200-year record of permafrost dynamics and carbon cycling in a collapse-scar bog, interior Alaska. Ecosystems, 16(1), 1-19.

Kaplan, F., Kopka, J., Haskell, D. W., Zhao, W., Schiller, K. C., Gatzke, N., ... & Guy, C. L. (2004). Exploring the temperature-stress metabolome of Arabidopsis. Plant physiology, 136(4), 4159-4168.

914 Keiluweit, M., Nico, P. S., Kleber, M., & Fendorf, S. (2016). Are oxygen limitations under recognized
915 regulators of organic carbon turnover in upland soils?. Biogeochemistry, 127(2), 157-171.
916
917 Keuper, F., Wild, B., Kummu, M., Beer, C., Blume-Werry, G., Fontaine, S., ... & Dorrepaal, E. (2020).
918 Carbon loss from northern circumpolar permafrost soils amplified by rhizosphere priming. Nature
919 Geoscience, 13(8), 560-565.
920
921 Kip, N., Dutilh, B. E., Pan, Y., Bodrossy, L., Neveling, K., Kwint, M. P., ... & Op den Camp, H. J.
922 (2011). Ultra - deep pyrosequencing of pmoA amplicons confirms the prevalence of
923 Methylomonas and Methylocystis in Sphagnum mosses from a Dutch peat bog. Environmental
924 microbiology reports, 3(6), 667-673.
925
926 Kujawinski, E. B., & Behn, M. D. (2006). Automated analysis of electrospray ionization Fourier
927 transform ion cyclotron resonance mass spectra of natural organic matter. Analytical chemistry,
928 78(13), 4363-4373.
929
930 Love, M. I., Huber, W., & Anders, S. (2014). Moderated estimation of fold change and dispersion for
931 RNA-seq data with DESeq2. Genome biology, 15(12), 550.
932
933 MATLAB (2022b). MathWorks. Version R2022a. Natick, Massachusetts: The MathWorks Inc.
934
935 LaRowe, D. E., & Van Cappellen, P. (2011). Degradation of natural organic matter: a thermodynamic
936 analysis. Geochimica et Cosmochimica Acta, 75(8), 2030-2042.
937
938 Malhotra, A., Brice, D. J., Childs, J., Graham, J. D., Hobbie, E. A., Vander Stel, H., ... & Iversen, C. M.
939 (2020). Peatland warming strongly increases fine-root growth. Proceedings of the National
940 Academy of Sciences, 117(30), 17627-17634.
941
942 McGivern, B. B., Cronin, D. R., Ellenbogen, J. B., Borton, M. A., Knutson, E. L., Freire-Zapata, V., ... &
943 Wrighton, K. C. (2024). Microbial polyphenol metabolism is part of the thawing permafrost
944 carbon cycle. Nature Microbiology, 9(6), 1454-1466.
945

McGivern, B. B., Ellenbogen, J. B., Hoyt, D. W., Bouranis, J. A., Stemple, B. P., Daly, R. A., ... & Wrighton, K. C. (2025). Polyphenol rewiring of the microbiome reduces methane emissions. The ISME Journal, 19(1), wraf108.

McPartland, M. Y., Montgomery, R. A., Hanson, P. J., Phillips, J. R., Kolka, R., & Palik, B. (2020). Vascular plant species response to warming and elevated carbon dioxide in a boreal peatland. Environmental Research Letters, 15(12), 124066.

Merritt, D. A., Hayes, J. M., & Marais, D. J. D. (1995). Carbon isotopic analysis of atmospheric methane by isotope - ratio - monitoring gas chromatography - mass spectrometry. Journal of Geophysical Research: Atmospheres, 100(D1), 1317-1326.

Minor, E. C., Steinbring, C. J., Longnecker, K., & Kujawinski, E. B. (2012). Characterization of dissolved organic matter in Lake Superior and its watershed using ultrahigh resolution mass spectrometry. Organic geochemistry, 43, 1-11.

Natali, S. M., Schuur, E. A., & Rubin, R. L. (2012). Increased plant productivity in Alaskan tundra as a result of experimental warming of soil and permafrost. Journal of ecology, 100(2), 488-498.

Nichols, J. E., & Peteet, D. M. (2019). Rapid expansion of northern peatlands and doubled estimate of carbon storage. Nature Geoscience, 12(11), 917-921.

Nobu, M. K., Narihiro, T., Rinke, C., Kamagata, Y., Tringe, S. G., Woyke, T., & Liu, W. T. (2015). Microbial dark matter ecogenomics reveals complex synergistic networks in a methanogenic bioreactor. The ISME journal, 9(8), 1710-1722.

Norby RJ, Childs J. 2018. SPRUCE: *Sphagnum* Productivity and Community Composition in the SPRUCE Experimental Plots**.** Oak Ridge National Laboratory, TES SFA, U.S. Department of Energy, Oak Ridge, Tennessee, U.S.A. https://doi.org/10.25581/spruce.049/1426474

Norby, R. J., Childs, J., Hanson, P. J., & Warren, J. M. (2019). Rapid loss of an ecosystem engineer: Sphagnum decline in an experimentally warmed bog. Ecology and Evolution, 9(22), 12571-12585.

Ofiti, N. O., Schmidt, M. W., Abiven, S., Hanson, P. J., Iversen, C. M., Wilson, R. M., ... & Malhotra, A. (2023). Climate warming and elevated CO2 alter peatland soil carbon sources and stability. Nature communications, 14(1), 7533.

Ogiso, T., Ueno, C., Dianou, D., Huy, T. V., Katayama, A., Kimura, M., & Asakawa, S. (2012). Methylomonas koyamae sp. nov., a type I methane-oxidizing bacterium from floodwater of a rice paddy field. International journal of systematic and evolutionary microbiology, 62(Pt_8), 1832-1837.

OpenAI. (2023). ChatGPT (Mar 14 version) [Large language model]. https://chat.openai.com/chat

Oswald, K., Graf, J. S., Littmann, S., Tienken, D., Brand, A., Wehrli, B., ... & Milucka, J. (2017). Crenothrix are major methane consumers in stratified lakes. The ISME journal, 11(9), 2124-2140.

Pankratov, T. A., & Dedysh, S. N. (2010). Granulicella paludicola gen. nov., sp. nov., Granulicella pectinivorans sp. nov., Granulicella aggregans sp. nov. and Granulicella rosea sp. nov., acidophilic, polymer-degrading acidobacteria from Sphagnum peat bogs. International Journal of Systematic and Evolutionary Microbiology, 60(12), 2951-2959.

Palozzi, J. E., & Lindo, Z. (2017). Boreal peat properties link to plant functional traits of ecosystem engineers. Plant and Soil, 418(1), 277-291.

Petro, C., Carrell, A. A., Wilson, R. M., Duchesneau, K., Noble - Kuchera, S., Song, T., ... & Kostka, J. E. (2023). Climate drivers alter nitrogen availability in surface peat and decouple N2 fixation from CH4 oxidation in the Sphagnum moss microbiome. Global Change Biology, 29(11), 3159-3176.

Phillips, J.R.,P.J. Hanson, and J.M. Warren. 2021.SPRUCE Plant Tissue Analyses Beginning 2017. Oak Ridge National Laboratory, TES SFA, U.S. Department of Energy, Oak Ridge, Tennessee, U.S.A. https://doi.org/10.25581/spruce.090/1780604

Podosokorskaya, O. A., Bonch-Osmolovskaya, E. A., Novikov, A. A., Kolganova, T. V., & Kublanov, I. V. (2013). Ornatilinea apprima gen. nov., sp. nov., a cellulolytic representative of the class

Anaerolineae. International Journal of Systematic and Evolutionary Microbiology, 63(Pt_1), 86-92.

Quast, C., Pruesse, E., Yilmaz, P., Gerken, J., Schweer, T., Yarza, P., ... & Glöckner, F. O. (2013). The SILVA ribosomal RNA gene database project: improved data processing and web-based tools. Nucleic Acids Res41 (D1): D590–D596.

Rawat, S. R., Männistö, M. K., Starovoytov, V., Goodwin, L., Nolan, M., Hauser, L., ... & Häggblom, M. M. (2014). Complete genome sequence of Granulicella tundricola type strain MP5ACTX9T, an Acidobacteria from tundra soil. Standards in genomic sciences, 9(3), 449-461.

R Core Team (2021). R: A language and environment for statistical ## computing. R Foundation for Statistical Computing, Vienna, Austria. ## URL https://www.R-project.org/.

Rintoul, S. R., Chown, S. L., DeConto, R. M., England, M. H., Fricker, H. A., Masson-Delmotte, V., ... & Xavier, J. C. (2018). Choosing the future of Antarctica. Nature, 558(7709), 233-241.

Salcher, M. M., Neuenschwander, S. M., Posch, T., & Pernthaler, J. (2015). The ecology of pelagic freshwater methylotrophs assessed by a high-resolution monitoring and isolation campaign. The ISME journal, 9(11), 2442-2453.

Salmon, V. G., Brice, D. J., Bridgham, S., Childs, J., Graham, J., Griffiths, N. A., ... & Hanson, P. J. (2021). Nitrogen and phosphorus cycling in an ombrotrophic peatland: a benchmark for assessing change. Plant and Soil, 466, 649-674.

Schmidt, O., Hink, L., Horn, M. A., & Drake, H. L. (2016). Peat: home to novel syntrophic species that feed acetate-and hydrogen-scavenging methanogens. The ISME journal, 10(8), 1954-1966.

Sebestyen, S. D., & Griffiths, N. A. (2016). SPRUCE enclosure corral and sump system: Description, operation, and calibration. Climate Change Science Institute, Oak Ridge National Laboratory, US Department of Energy, Oak Ridge, TN. doi: http://dx. doi. org/10.3334/CDIAC/spruce, 30.

Sebestyen, S. D., Lany, N. K., Roman, D. T., Burdick, J. M., Kyllander, R. L., Verry, E. S., & Kolka, R. K. (2021). Hydrological and meteorological data from research catchments at the Marcell Experimental Forest, Minnesota, USA. Hydrological Processes, 35(3), e14092.

Shannon P, Markiel A, Ozier O, et al. (2003). Cytoscape: a software environment for integrated models of biomolecular interaction networks. Genome Res. 13(11): 2498–2504. [doi:10.1101/gr.1239303].

Spinelli, F., Cellini, A., Marchetti, L., Nagesh, K. M., & Piovene, C. (2011). Emission and function of volatile organic compounds in response to abiotic stress. In A. Shanker & B. Venkateswarlu (Eds.), Abiotic stress in plants—Mechanisms and adaptations [Book chapter].

Stingl, U., Radek, R., Yang, H., & Brune, A. (2005). "Endomicrobia": cytoplasmic symbionts of termite gut protozoa form a separate phylum of prokaryotes. Applied and Environmental Microbiology, 71(3), 1473-1479.

Stoecker, K., Bendinger, B., Schöning, B., Nielsen, P. H., Nielsen, J. L., Baranyi, C., ... & Wagner, M. (2006). Cohn's Crenothrix is a filamentous methane oxidizer with an unusual methane monooxygenase. Proceedings of the national academy of sciences, 103(7), 2363-2367.

Sutton-Grier, A. E., & Megonigal, J. P. (2011). Plant species traits regulate methane production in freshwater wetland soils. Soil Biology and Biochemistry, 43(2), 413-420.

Synytsya, A., Čopíková, J., Matějka, P., & Machovič, V. J. C. P. (2003). Fourier transform Raman and infrared spectroscopy of pectins. Carbohydrate polymers, 54(1), 97-106.

Tfaily, M. M., Hamdan, R., Corbett, J. E., Chanton, J. P., Glaser, P. H., & Cooper, W. T. (2013). Investigating dissolved organic matter decomposition in northern peatlands using complimentary analytical techniques. Geochimica et Cosmochimica Acta, 112, 116-129.

Tfaily, M. M., Cooper, W. T., Kostka, J. E., Chanton, P. R., Schadt, C. W., Hanson, P. J., ... & Chanton, J. P. (2014). Organic matter transformation in the peat column at Marcell Experimental Forest: humification and vertical stratification. Journal of Geophysical Research: Biogeosciences, 119(4), 661-675.

Tolic, N., et al. Formularity: software for automated formula assignment of natural and other organic matter from ultrahigh-resolution mass spectra. Analytical Chemistry. 89 (23), 12659-12665 (2017).

Treat, C. C., Wollheim, W. M., Varner, R. K., Grandy, A. S., Talbot, J., & Frolking, S. (2014). Temperature and peat type control CO 2 and CH 4 production in Alaskan permafrost peats. Global Change Biology, 20(8), 2674-2686.

Turetsky, M. R. (2003). The role of bryophytes in carbon and nitrogen cycling. The bryologist, 106(3), 395-409.

Turetsky, M. R., Wieder, R. K., Vitt, D. H., Evans, R. J., & Scott, K. D. (2007). The disappearance of relict permafrost in boreal north America: Effects on peatland carbon storage and fluxes. Global Change Biology, 13(9), 1922-1934.

Tveit, A. T., Urich, T., Frenzel, P., & Svenning, M. M. (2015). Metabolic and trophic interactions modulate methane production by Arctic peat microbiota in response to warming. Proceedings of the National Academy of Sciences, 112(19), E2507-E2516.

The MathWorks Inc. (2022). MATLAB version: 9.13.0 (R2022b), Natick, Massachusetts: The MathWorks Inc. https://www.mathworks.com

van Breemen, N. (1995). How Sphagnum bogs down other plants. Trends in ecology & evolution, 10(7), 270-275.

Verhoeven, J.T.A. & W.M. Liefveld. (1997). The ecological significance of organochemical compounds in Sphagnum. *Acta botanica neerlandica*, *46*(2), 117–130.

Verbeke, B. A., Lamit, L. J., Lilleskov, E. A., Hodgkins, S. B., Basiliko, N., Kane, E. S., ... & Chanton, J. P. (2022). Latitude, elevation, and mean annual temperature predict peat organic matter chemistry at a global scale. *Global Biogeochemical Cycles*, *36*(2), e2021GB007057.

Wang, H., Richardson, C. J., & Ho, M. (2015). Dual controls on carbon loss during drought in peatlands. Nature Climate Change, 5(6), 584-587.

Wang, H. Z., Yan, Y. C., Gou, M., Yi, Y., Xia, Z. Y., Nobu, M. K., ... & Tang, Y. Q. (2019). Response of propionate-degrading methanogenic microbial communities to inhibitory conditions. Applied Biochemistry and Biotechnology, 189(1), 233-248.

Wang, Y., Gabbard, H.D., and Pai, P. (1991). Inhibition of acetate methanogenesis by phenols. J. Environ. Eng. 117. doi: 10.1061/(ASCE)0733-9372(1991)117:4(487)

Wang, H., Tian, J., Chen, H., Ho, M., Vilgalys, R., Bu, Z. J., ... & Richardson, C. J. (2021). Vegetation and microbes interact to preserve carbon in many wooded peatlands. Communications Earth & Environment, 2(1), 1-8.

Wardle, R., & Smith, I. (2004). Modeled response of the Australian monsoon to changes in land surface temperatures. Geophysical Research Letters, 31(16).

Whiticar, M. J. (1999). Carbon and hydrogen isotope systematics of bacterial formation and oxidation of methane. Chemical Geology, 161(1-3), 291-314.

Wilson, R. M., Hopple, A. M., Tfaily, M. M., Sebestyen, S. D., Schadt, C. W., Pfeifer-Meister, L., ... & Hanson, P. J. (2016). Stability of peatland carbon to rising temperatures. Nature Communications, 7(1), 1-10.

Wilson, R. M., & Tfaily, M. M. (2018). Advanced molecular techniques provide new rigorous tools for characterizing organic matter quality in complex systems. Journal of Geophysical Research: Biogeosciences, 123(6), 1790-1795.

Wilson, R. M., Tfaily, M. M., Kolton, M., Johnston, E. R., Petro, C., Zalman, C. A., ... & Kostka, J. E. (2021a). Soil metabolome response to whole-ecosystem warming at the Spruce and Peatland Responses under Changing Environments experiment. Proceedings of the National Academy of Sciences, 118(25).

Wilson, R. M., Griffiths, N. A., Visser, A., McFarlane, K. J., Sebestyen, S. D., Oleheiser, K. C., ... & Chanton, J. P. (2021b). Radiocarbon analyses quantify peat carbon losses with increasing temperature in a whole ecosystem warming experiment. Journal of Geophysical Research: Biogeosciences, 126(11), e2021JG006511.

Wilson, R.M., Hough, M.A., Verbeke, B.A., Hodgkins, S.B., *Isogenie Coordinators*, Chanton, J.P., Saleska, S.D., Rich, V.I. and Tfaily, M.M. (2022) Plant organic matter inputs exert a strong

control on soil organic matter decomposition in a thawing permafrost peatland. Science of the Total Environment, 820, 152757.

Wilkins, M. J., Kennedy, D. W., Castelle, C. J., Field, E. K., Stepanauskas, R., Fredrickson, J. K., & Konopka, A. E. (2014). Single-cell genomics reveals metabolic strategies for microbial growth and survival in an oligotrophic aquifer. Microbiology, 160(2), 362-372.

Zalman, C.A., Meade, N., Chanton, J., Kostka, J.E., Bridgham, S.D., & Keller, J.K. (2018) Methylotrophic methanogenesis in *Sphagnum*-dominated peatland soils. Soil Biology and Biochemistry 188, 156-160.

Zhang, Y., Zheng, N., Wang, J., Yao, H., Qiu, Q., & Chapman, S. J. (2019). High turnover rate of free phospholipids in soil confirms the classic hypothesis of PLFA methodology. Soil Biology and Biochemistry, 135, 323-330.

Zheng, H., Dietrich, C., Radek, R., & Brune, A. (2016). E ndomicrobium proavitum, the first isolate of E ndomicrobia class. nov.(phylum E lusimicrobia)–an ultramicrobacterium with an unusual cell cycle that fixes nitrogen with a G roup IV nitrogenase. Environmental Microbiology, 18(1), 191-204.

Figure1.

Hypothesis:

Plant inputs

polysaccharides, glycosides, phenols, lignins, aromatics, proteins, fatty acids

Porewater composition

aminosugars, lignin, phospholipids, phenolics, phytochemicals, oxidized aromatics

C gas production

CO_2, CH_4, $\delta^{13}CH_4$, $\delta^{13}CO_2$

Figure2.

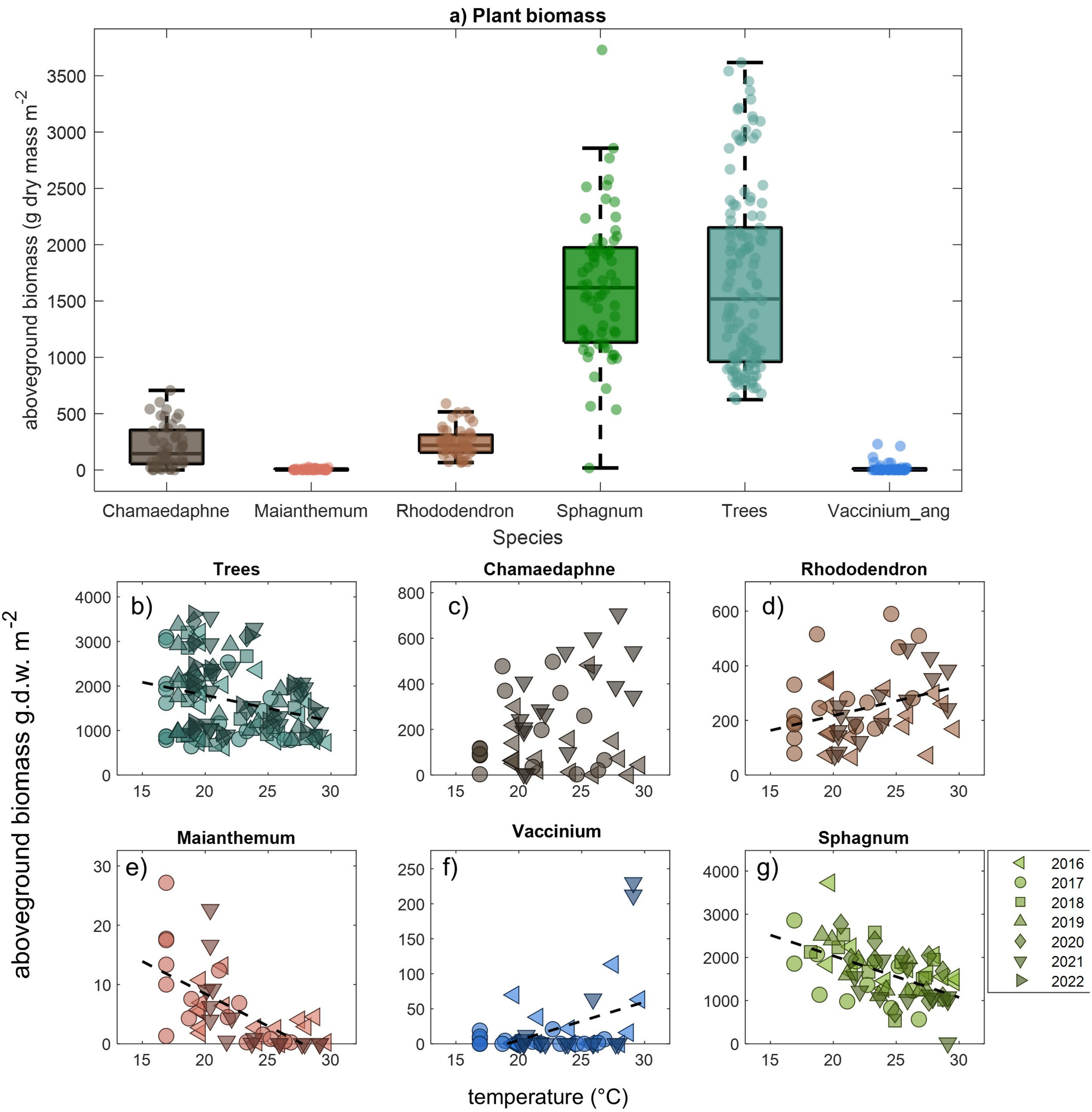
a) Plant biomass
aboveground biomass (g dry mass m-2
3500
3000
2500
2000
1500
1000
500
0
Chamaedaphne
Maianthemum
Rhododendron
Sphagnum
Trees
Vaccinium_ang
Species
aboveground biomass g.d.w. m-2
Trees
b)
Chamaedaphne
c)
Rhododendron
d)
Maianthemum
e)
Vaccinium
f)
Sphagnum
g)
2016
2017
2018
2019
2020
2021
2022
temperature (°C)

Figure3.

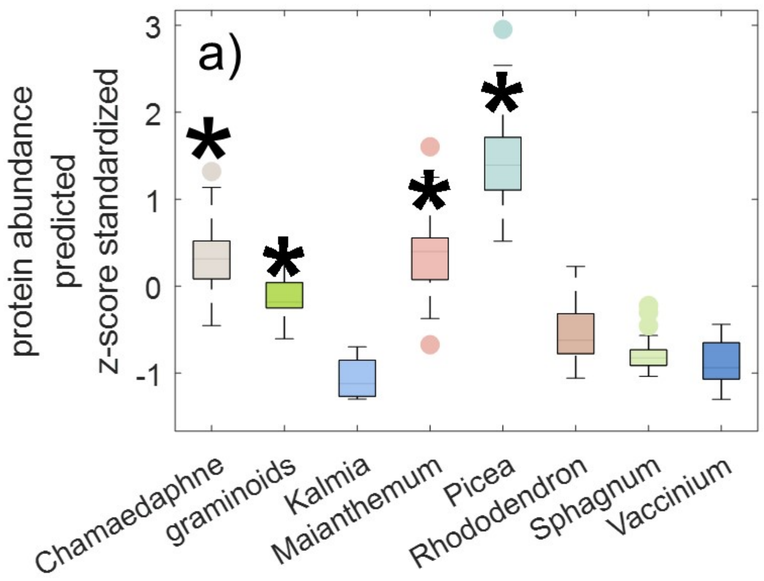
a)
protein abundance
predicted
z-score standardized
3
2
1
0
-1
Chamaedaphne
graminoids
Kalmia
Maianthemum
Picea
Rhododendron
Sphagnum
Vaccinium

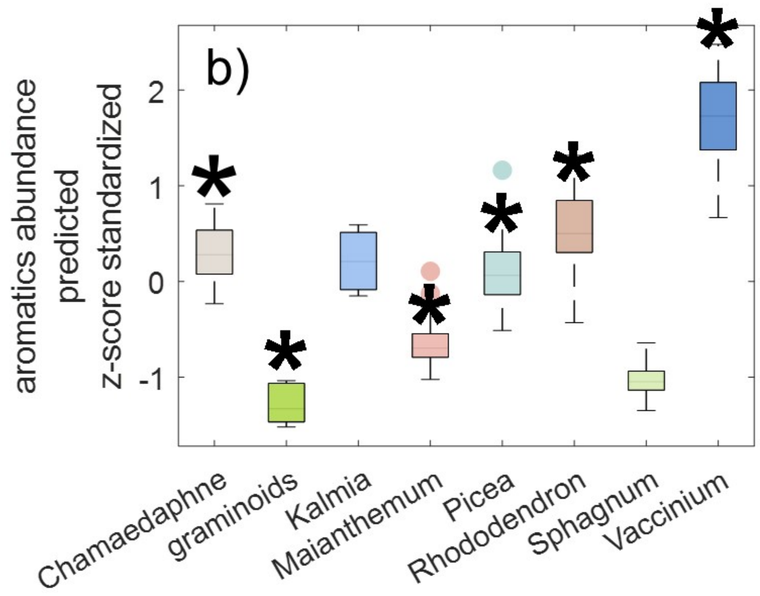
b)
aromatics abundance
predicted
z-score standardized
2
1
0
-1
Chamaedaphne
graminoids
Kalmia
Maianthemum
Picea
Rhododendron
Sphagnum
Vaccinium

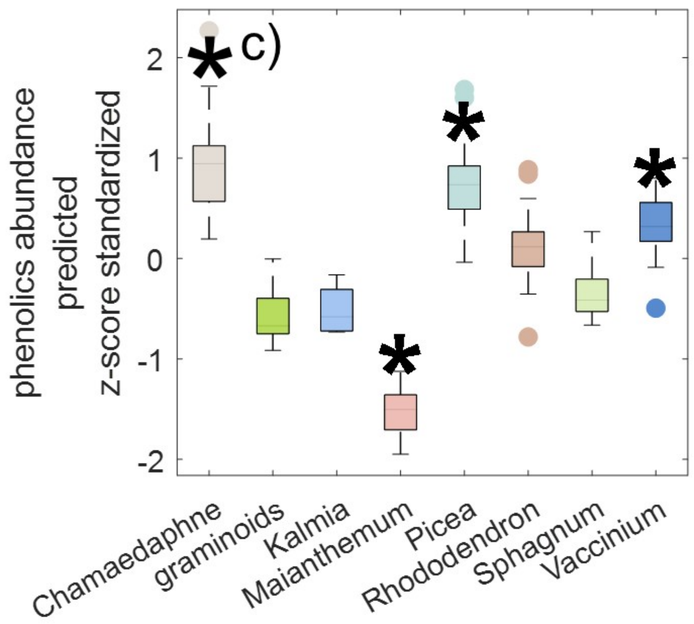
c)
phenolics abundance
predicted
z-score standardized
2
1
0
-1
-2
Chamaedaphne
graminoids
Kalmia
Maianthemum
Picea
Rhododendron
Sphagnum
Vaccinium

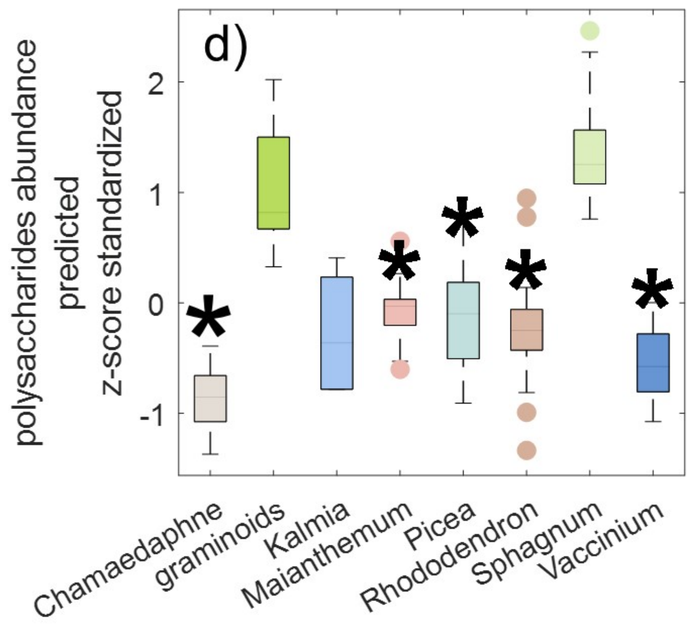
d)
polysaccharides abundance
predicted
z-score standardized
2
1
0
-1
Chamaedaphne
graminoids
Kalmia
Maianthemum
Picea
Rhododendron
Sphagnum
Vaccinium

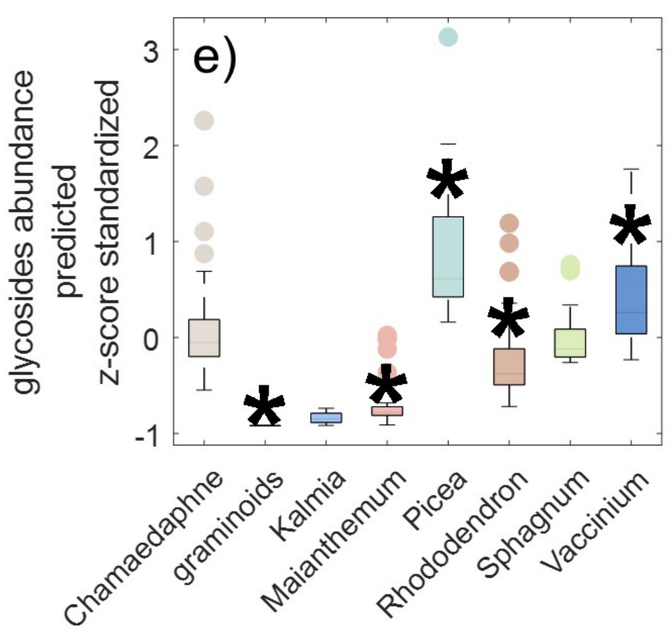
e)
glycosides abundance
predicted
z-score standardized
3
2
1
0
-1
Chamaedaphne
graminoids
Kalmia
Maianthemum
Picea
Rhododendron
Sphagnum
Vaccinium

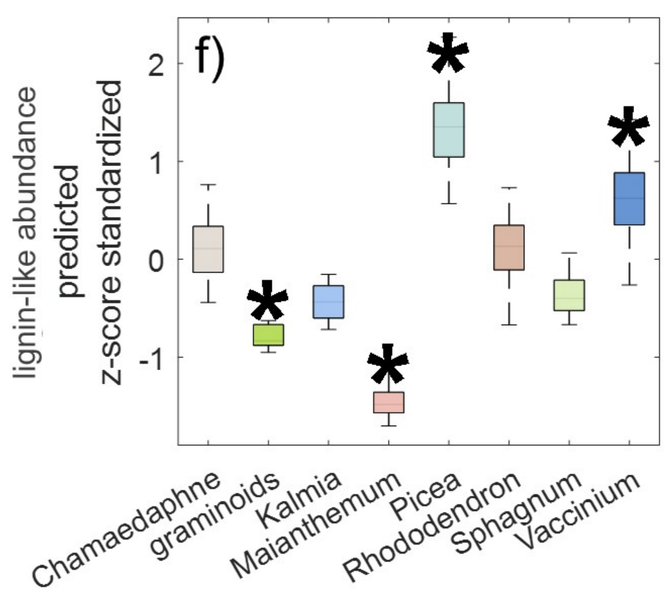
f)
lignin-like abundance
predicted
z-score standardized
2
1
0
-1
Chamaedaphne
graminoids
Kalmia
Maianthemum
Picea
Rhododendron
Sphagnum
Vaccinium

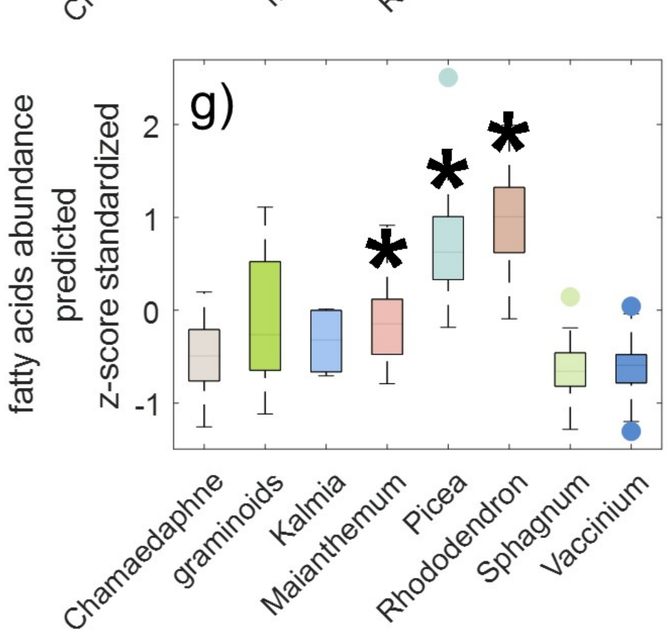
g)
fatty acids abundance
predicted
z-score standardized
2
1
0
-1
Chamaedaphne
graminoids
Kalmia
Maianthemum
Picea
Rhododendron
Sphagnum
Vaccinium

Figure4.

Maianthemum

Picea

Rhododendron

Chaemadaphne

fatty acids

proteins

phenolics

polysaccharides

aromatics

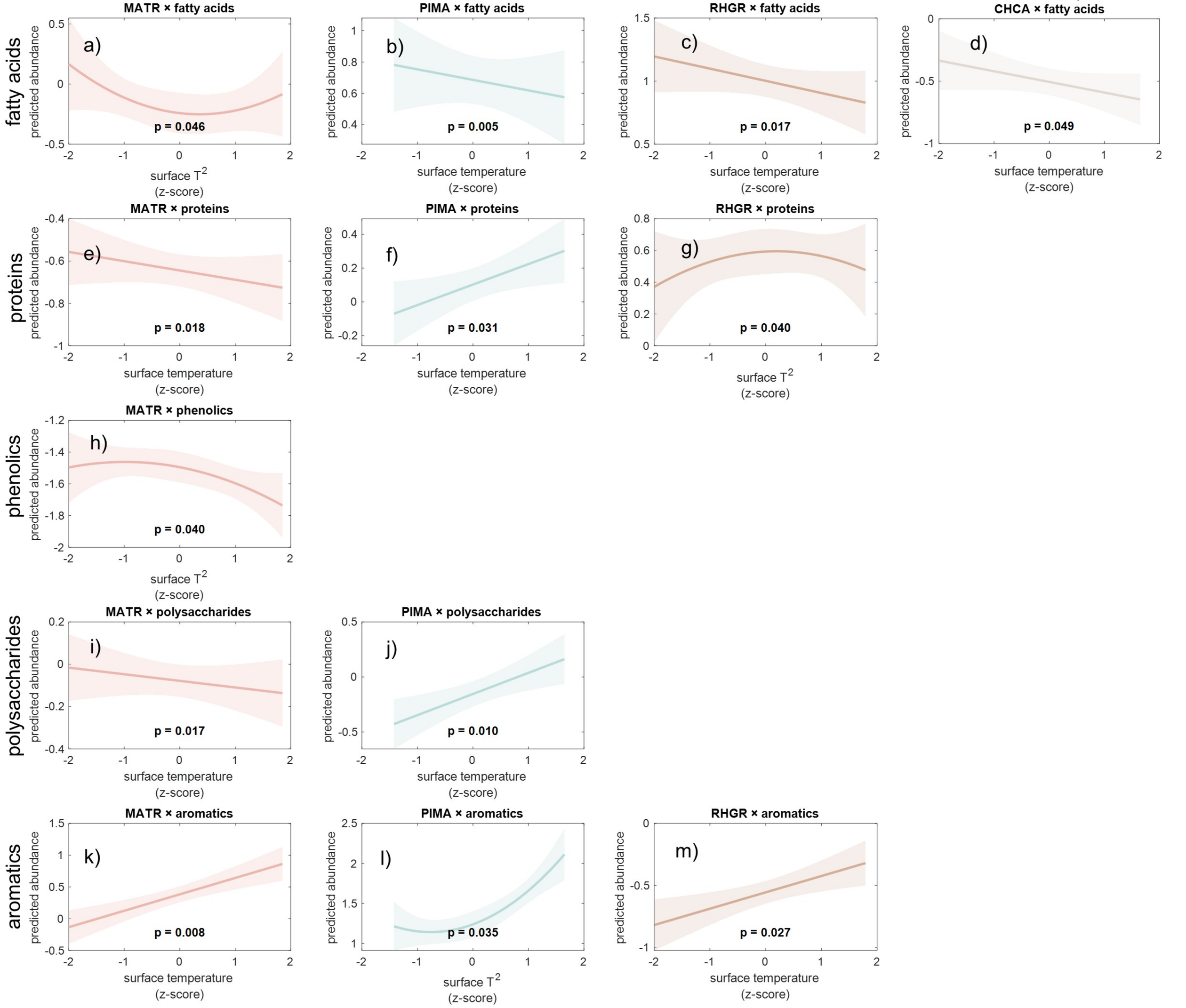

Figure5.

Predicted Abundances vs. Temperature

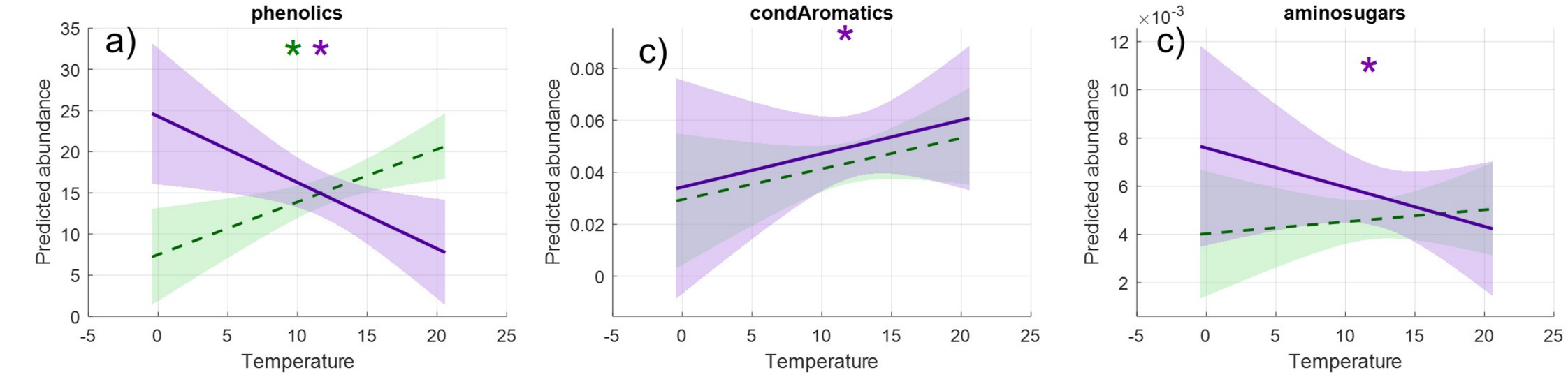

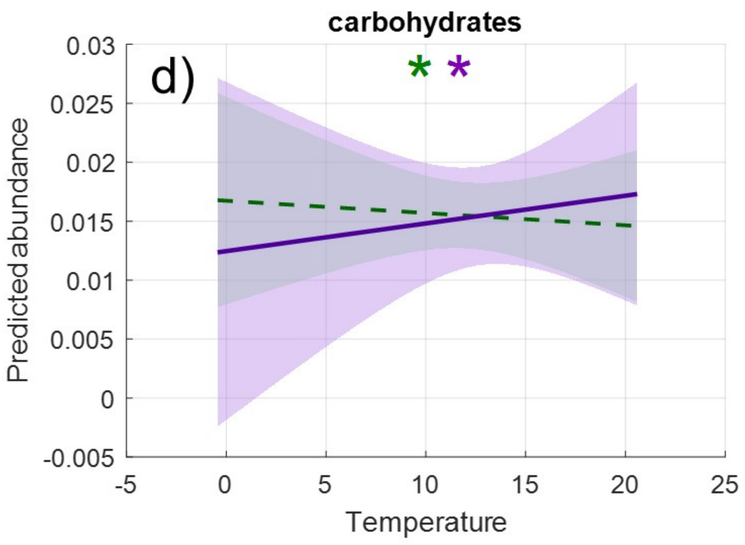

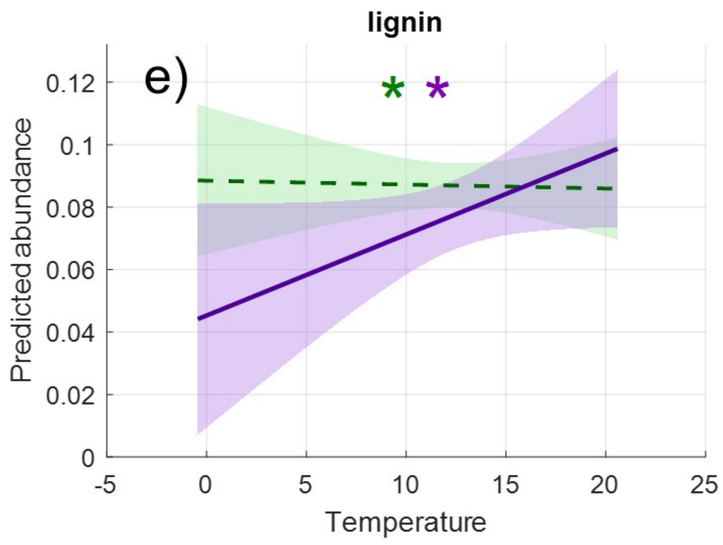

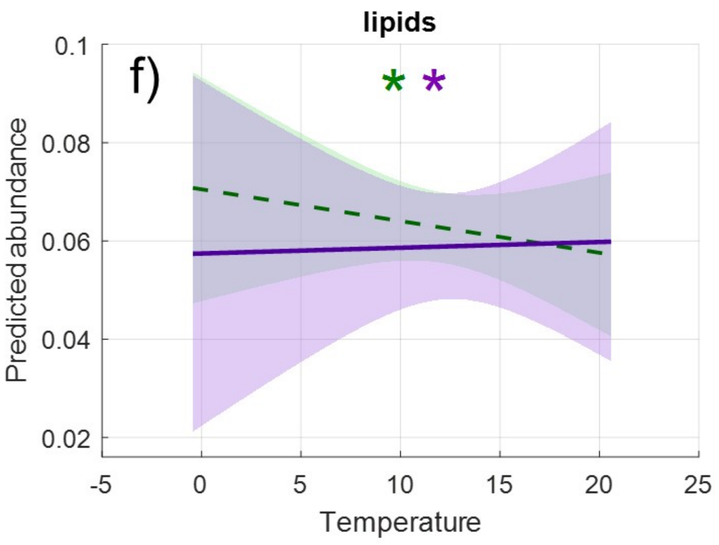

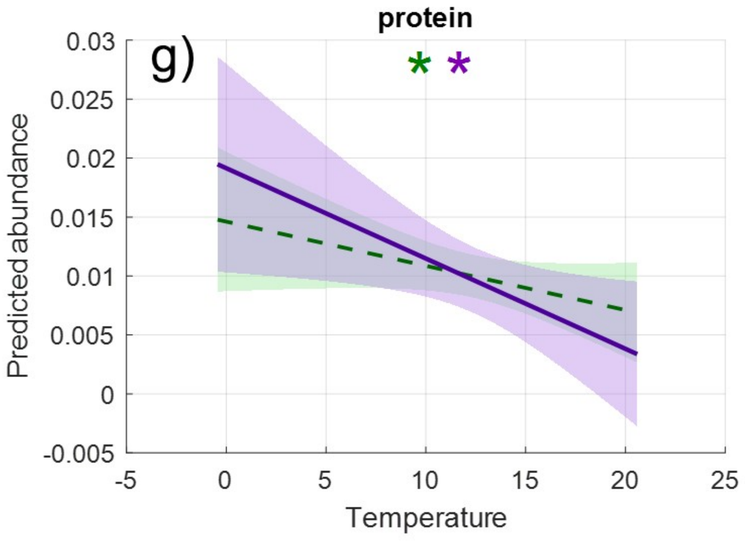

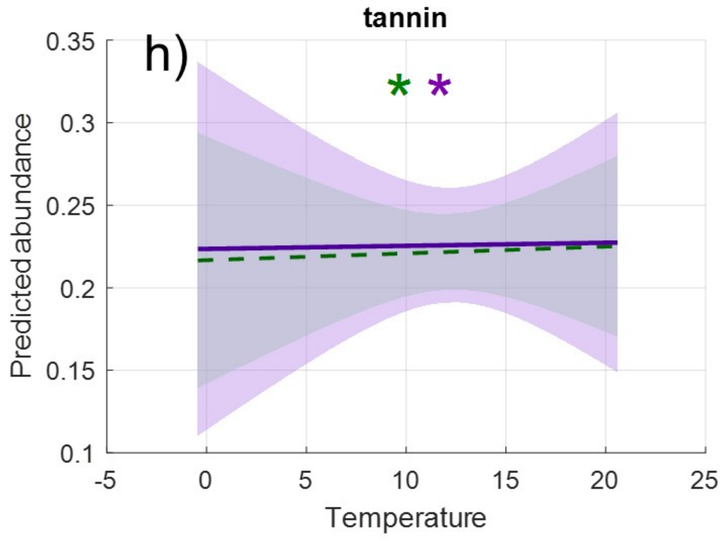

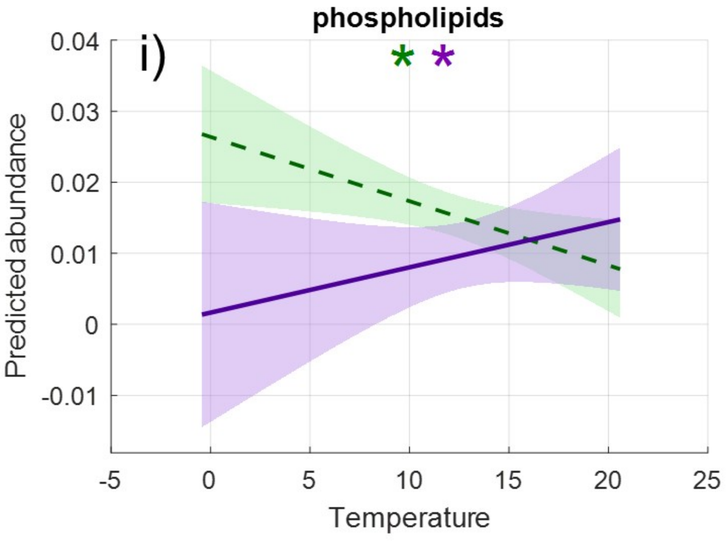

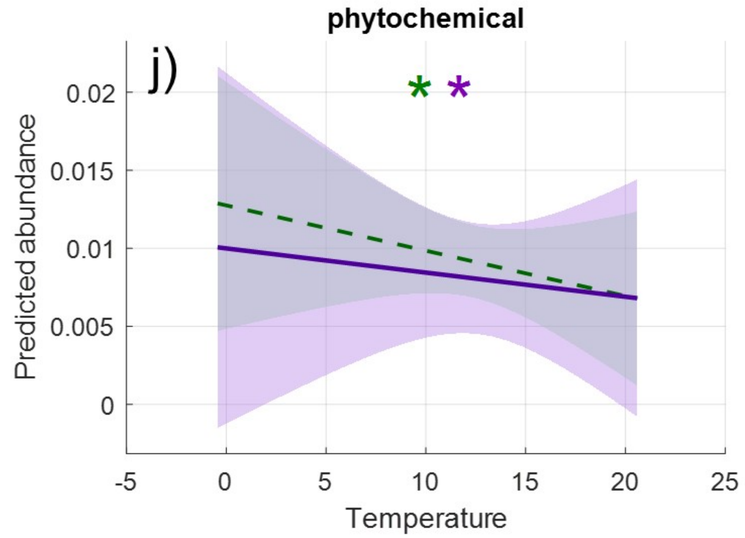

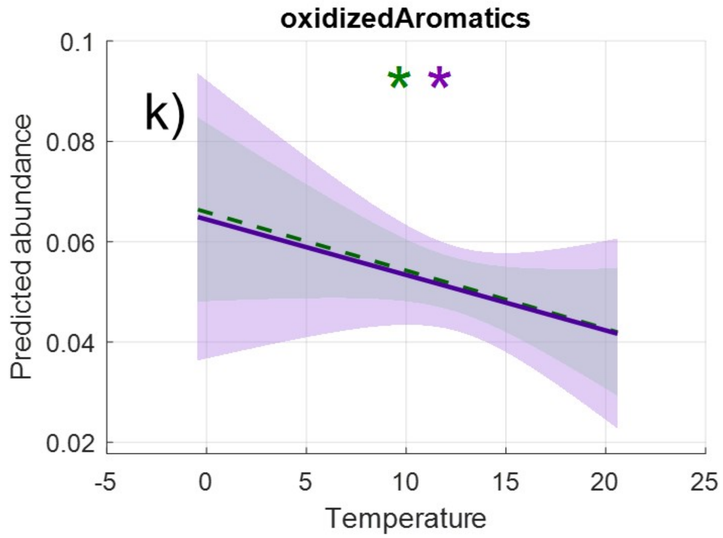

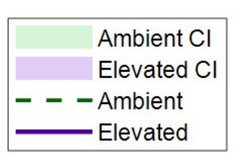

Figure6.

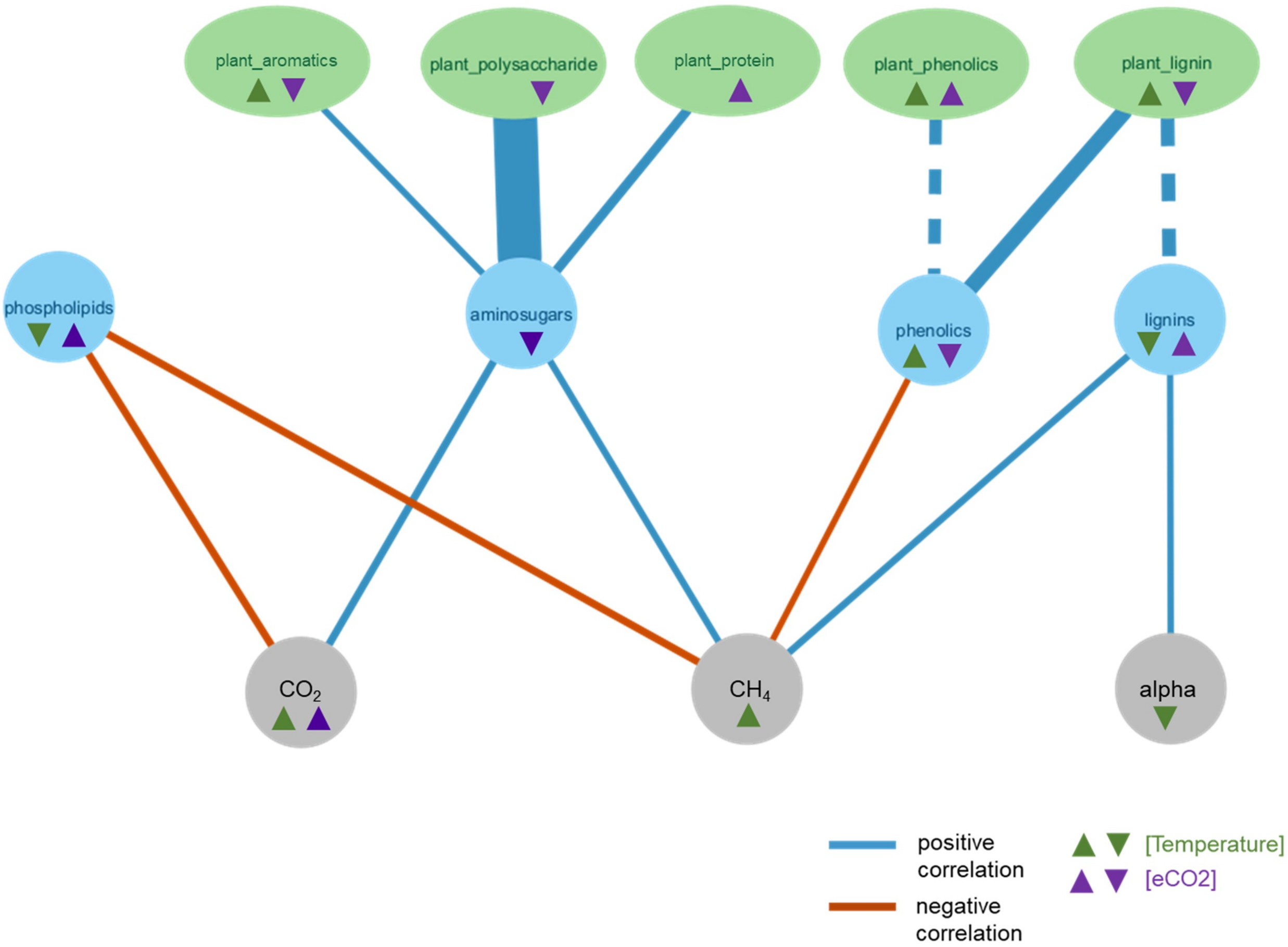
plant_aromatics
plant_polysaccharide
plant_protein
plant_phenolics
plant_lignin
phospholipids
aminosugars
phenolics
lignins
CO_2
CH_4
alpha
positive correlation
negative correlation
[Temperature]
[eCO2]

Figure7.

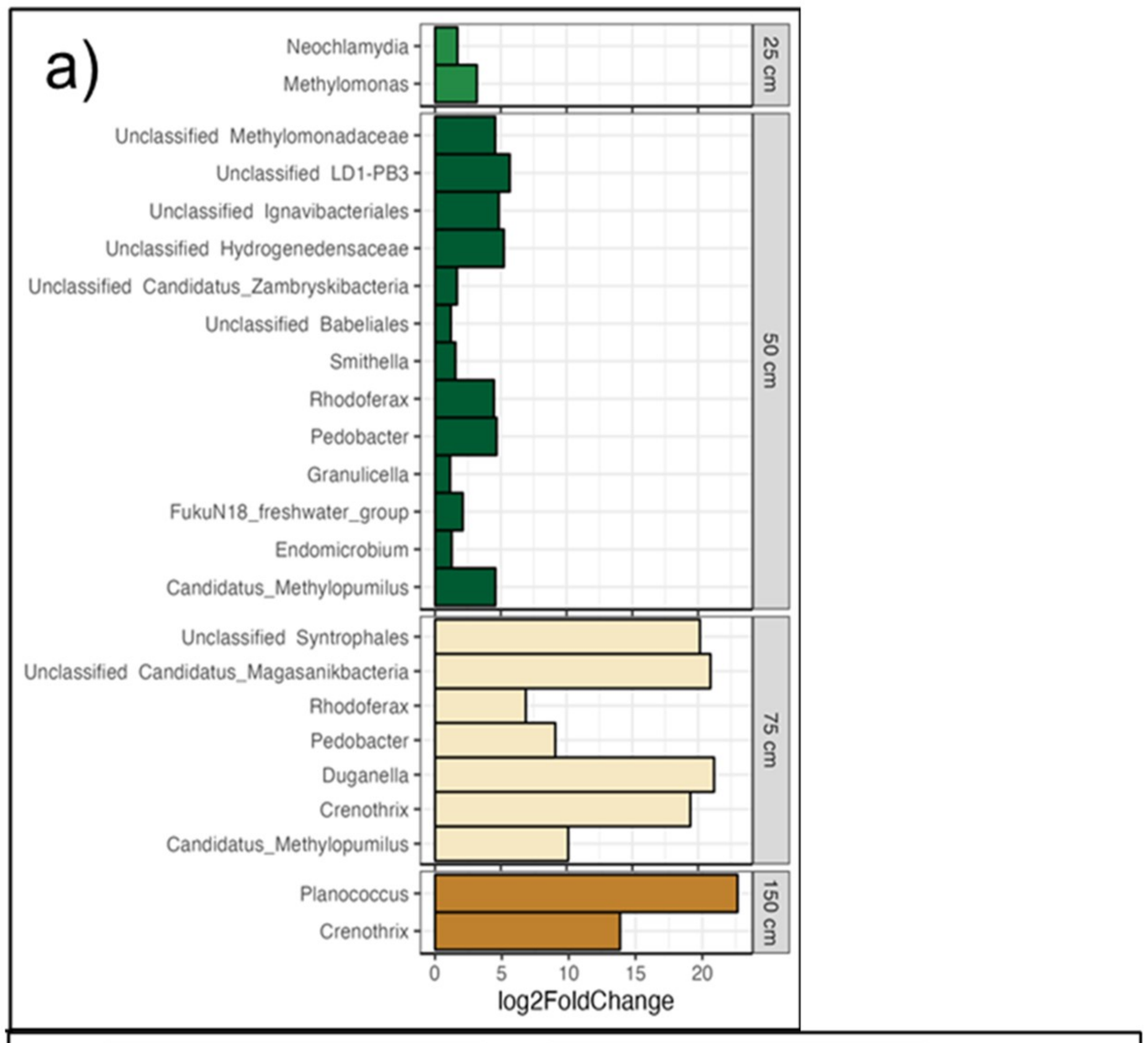
a)
Neochlamydia
Methylomonas
Unclassified Methylomonadaceae
Unclassified LD1-PB3
Unclassified Ignavibacteriales
Unclassified Hydrogenedensaceae
Unclassified Candidatus_Zambryskibacteria
Unclassified Babeliales
Smithella
Rhodoferax
Pedobacter
Granulicella
FukuN18_freshwater_group
Endomicrobium
Candidatus_Methylopumilus
Unclassified Syntrophales
Unclassified Candidatus_Magasanikbacteria
Rhodoferax
Pedobacter
Duganella
Crenothrix
Candidatus_Methylopumilus
Planococcus
Crenothrix
25 cm
50 cm
75 cm
150 cm
0
5
10
15
20
log2FoldChange

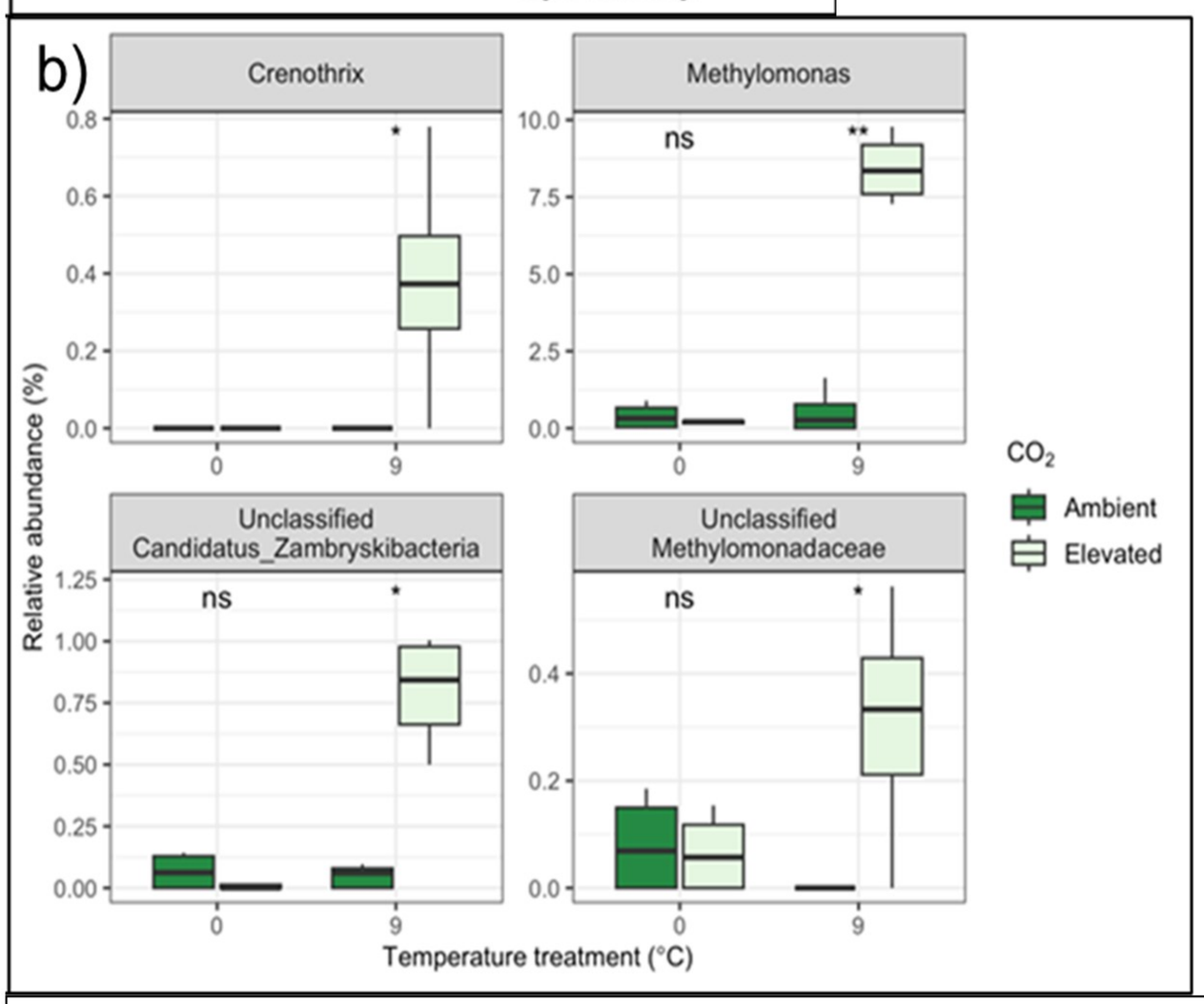
b)
Crenothrix
Methylomonas
Unclassified Candidatus_Zambryskibacteria
Unclassified Methylomonadaceae
ns
*
**
Relative abundance (%)
0
9
Temperature treatment (°C)
CO2
Ambient
Elevated

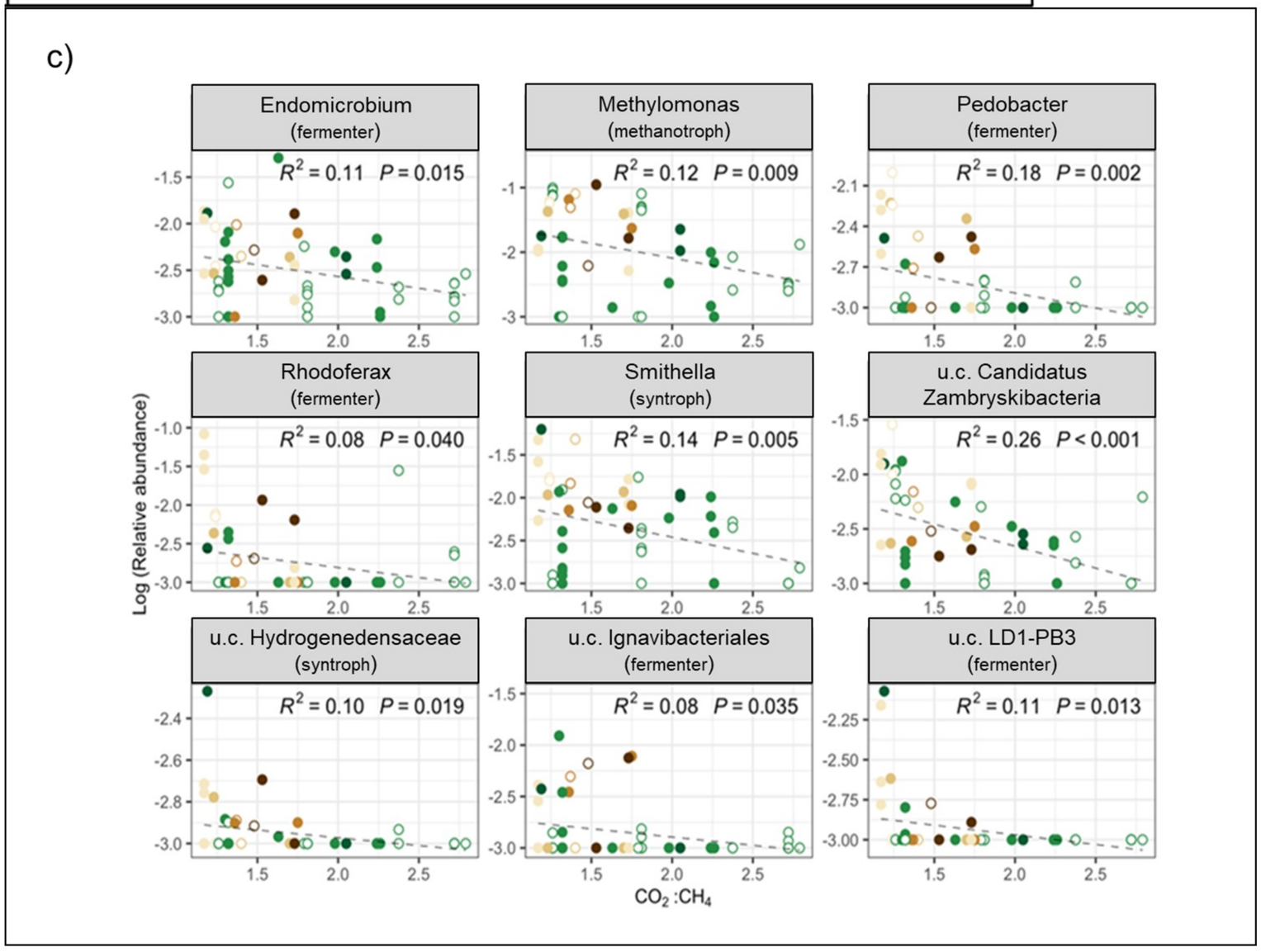
c)
Endomicrobium (fermenter)
Methylomonas (methanotroph)
Pedobacter (fermenter)
Rhodoferax (fermenter)
Smithella (syntroph)
u.c. Candidatus Zambryskibacteria
u.c. Hydrogenedensaceae (syntroph)
u.c. Ignavibacteriales (fermenter)
u.c. LD1-PB3 (fermenter)
R2 = 0.11 P = 0.015
R2 = 0.12 P = 0.009
R2 = 0.18 P = 0.002
R2 = 0.08 P = 0.040
R2 = 0.14 P = 0.005
R2 = 0.26 P < 0.001
R2 = 0.10 P = 0.019
R2 = 0.08 P = 0.035
R2 = 0.11 P = 0.013
Log (Relative abundance)
CO2 :CH4